J. Cell. Mol. Med. Vol 13, No 8B, 2009 pp. 2083-2108

A pro-inflammatory signature mediates FGF2-induced angiogenesis

Germán Andrés [a], Daria Leali [a], Stefania Mitola [a], Daniela Coltrini [a], Maura Camozzi [a], Michela Corsini [a], Mirella Belleri [a], Emilio Hirsch [b], Reto A. Schwendener [c], Gerhard Christofori [d], Antonio Alcamí [e], Marco Presta [a, *]

[a] Unit of General Pathology and Immunology, Department of Biomedical Sciences and Biotechnology, School of Medicine, University of Brescia, Brescia, Italy
[b] Department of Genetics, Biology and Biochemistry, University of Turin, Turin, Italy
[c] Laboratory of Liposome Research, Institute of Molecular Cancer Research, University of Zurich, Zurich, Switzerland
[d] Institute of Biochemistry and Genetics, Department of Clinical Biological Sciences, University of Basel, Basel, Switzerland
[e] Centro de Biología Molecular Severo Ochoa (CSIC-UAM), Campus Universidad Autónoma, Cantoblanco, Madrid, Spain

Received: April 22, 2008; Accepted: June 23, 2008

Abstract

Fibroblast growth factor-2 (FGF2) is a potent angiogenic growth factor. Here, gene expression profiling of FGF2-stimulated microvascular endothelial cells revealed, together with a prominent pro-angiogenic profile, a pro-inflammatory signature characterized by the up-regulation of pro-inflammatory cytokine/chemokines and their receptors, endothelial cell adhesion molecules and members of the eicosanoid pathway. Real-time quantitative PCR demonstrated early induction of most of the FGF2-induced, inflammation-related genes. Accordingly, chick embryo chorioallantoic membrane (CAM) and murine Matrigel plug angiogenesis assays demonstrated a significant monocyte/macrophage infiltrate in the areas of FGF2-driven neovascularization. Similar results were obtained when the conditioned medium (CM) of FGF2-stimulated endothelial cells was delivered onto the CAM, suggesting that FGF2-upregulated chemoattractants mediate the inflammatory response. Importantly, FGF2-triggered new blood vessel formation was significantly reduced in *phosphatidylinositol 3-kinase*-γ null mice exhibiting defective leucocyte migration or in clodronate liposome-treated, macrophage-depleted mice. Furthermore, the viral pan-chemokine antagonist M3 inhibited the angiogenic and inflammatory responses induced by the CM of FGF2-stimulated endothelial cells and impaired FGF2-driven neovascularization in the CAM assay. These findings point to inflammatory chemokines as early mediators of FGF2-driven angiogenesis and indicate a non-redundant role for inflammatory cells in the neovascularization process elicited by the growth factor.

Keywords: angiogenesis • chemokines • FGF • inflammation • macrophages

Introduction

Angiogenesis and inflammation are closely integrated processes in a number of physiological and pathological conditions, including wound healing, psoriasis, diabetic retinopathy, rheumatoid arthritis, arteriosclerosis and cancer [1, 2]. Inflammatory cells may produce angiogenic cytokines, growth factors and proteases that contribute to the formation of new vascular structures at the site of inflammation, tissue damage or tumour growth [3]. Conversely, microvascular endothelium activated by a number of cytokines and angiogenic growth factors can express pro-inflammatory molecules involved in leucocyte recruitment and activation [4, 5]. Strikingly, neovascularization and inflammation share a number of common signalling pathways and molecular mediators, the cyclooxygenase (Cox)/prostaglandin pathway representing a paradigm of this convergence [6]. Also, various chemokines may act both as leucocyte attractants and as angiogenic inducers by acting directly on endothelial cells [7]. Moreover, a number of pro-inflammatory cytokines [*e.g.* interleukin-1α (IL-1α), IL-1β, IL-6,

*Correspondence to: Marco PRESTA,
General Pathology, Department of Biomedical Sciences and Biotechnology, University of Brescia, Viale Europa 11, 25123 Brescia, Italy.
Tel.: 139-030-3717311
Fax: 139-030-3701157
E-mail: presta@med.unibs.it

doi:10.1111/j.1582-4934.2008.00415.x

tumour necrosis factor-α (TNFα), high mobility group box-1 (HMGB1) and osteopontin (Opn)] may induce blood vessel formation *via* direct engagement of target endothelial cells or indirectly by inducing leucocytes and/or endothelial cells to produce pro-angiogenic mediators [8–10]. Conversely, the angiogenic factors vascular endothelial growth factor (VEGF) and angiopoietin-1 (Ang-1) may elicit pro-inflammatory responses in endothelial cells by up-regulating the expression of cell adhesion molecules and inflammatory mediators [11, 12].

Fibroblast growth factor 2 (FGF2) is a pleiotropic heparin-binding factor that promotes growth and differentiation of a broad spectrum of cell types [13]. FGF2 triggers a complex 'pro-angiogenic phenotype' in endothelial cells that recapitulates the neovascularization process and exerts a potent angiogenic response in a variety of *in vivo* animal models [13]. The angiogenic activity of FGF2 is mediated by its interaction with high-affinity tyrosine kinase FGF receptors (FGFRs) and low-affinity heparan sulphate proteoglycans and integrin receptors, leading to the activation of multiple signal transduction pathways, including phospholipase C-γ, phosphatidylinositol 3-kinase (PI3K) and mitogen-activated protein kinases [13, 14].

Elevated levels of FGF2 have been implicated in the pathogenesis of several diseases characterized by a deregulated angiogenic/inflammatory response, including cancer [13]. Inflammatory cells, including mononuclear phagocytes, T lymphocytes and mast cells, express FGF2. Moreover, FGF2 production and release from endothelial cells are triggered by inflammatory mediators (reviewed in [13]). Conversely, FGF2 may amplify the endothelial cell response to inflammatory stimuli [15] and up-regulates the expression of *Opn* [10], *Ccl2* chemokine [16] and *Cox-2* [17] in endothelial cells. Taken together, these observations point to the existence of a tight cross-talk between inflammatory and angiogenic responses during FGF2-driven neovascularization.

Here, we report that FGF2 induces a pro-inflammatory signature in murine microvascular endothelial cells. Consistently, we provide *in vivo* evidence about the non-redundant role of chemokines and infiltrating monocytes/macrophages in FGF2-driven neovascularization.

Materials and methods

Reagents and cells

Recombinant human FGF2 was purified as previously described [18]. Ketoprofen and hydrocortisone were purchased from Sigma-Aldrich (Saint Louis, MO, USA). Recombinant M3 protein was expressed in the baculovirus system and purified by affinity chromatography [19].

Murine lung microvascular endothelial cells (1G11 cells) [20] were obtained from A. Vecchi (Istituto Scientifico Humanitas, Rezzato, Milan, Italy) and cultured in Dulbecco modified Eagle medium (DMEM) containing 20% inactivated foetal bovine serum (FBS). Cells were usually starved for 24 hrs with DMEM containing 0.5% FBS before stimulation with FGF2. In all the assays, endotoxin content was lower than 0.06 EU/ml (6 pg/ml), as determined by the Limulus amebocyte lysate method (Cambrex BioSiences, Walkersville, MD, USA).

Affymetrix genechip analysis

Three independent 1G11 cell cultures were stimulated for 10 hrs with 30 ng/ml FGF2 in DMEM supplemented with 0.5% FBS. As a control reference, duplicate samples from non-treated cells were also analysed. RNA extraction, reverse transcription, cRNA preparation and GeneChip hybridization were performed according to the manufacturer's instructions (http://www.affymetrix.com/support/technical/manual/expression_manual.affx, Affymetrix, Santa Clara, CA, USA). Briefly, total RNA was extracted using Trizol (Invitrogen Life Technologies, Carlsbad, CA, USA) and phase lock gels (Eppendorf, Hamburg, Deutschland) and purified with Rneasy columns (Qiagen, Valencia, CA, USA). Ten micrograms of RNA were then used as a template for double-stranded cDNA synthesis primed using a T7-(dT)24 oligonucleotide. Double-stranded cDNA was then transcribed using T7 RNA polymerase to produce biotin-labelled cRNA. Resulting cRNA was fragmented and hybridized to Affymetrix GeneChip Murine Genome MOE430A oligonucleotide microarrays.

To define the transcriptional profile modulated by FGF2, raw expression measures at the probe level data were computed using robust multi-array average. Quantile normalization was performed across all microarrays to achieve the same distribution of signal intensities for each array [21]. Data analysis was then carried out using Genespring 7.3 software (Silicon Genetics, Redwood City, CA, USA). Initial data filtering of genes with a 'present' detection call in at least one chip, according to Affymetrix MAS5 algorithm, was applied. Differential expression was assessed by applying a twofold change cut-off and a Welch-modified two-sample t-test. A false discovery rate of 5% was used as a cut-off for statistical significance.

FGF2-regulated genes were annotated by employing the web-accessible software DAVID [22] (Database for Annotation, Visualization and Integrated Discovery; http://david.abcc.ncifcrf.gov/) and NetAffx Analysis Center (http://www.affymetrix.com/analysis/index.affx), which provides functional genomic annotations for gene ontology (GO), protein domain and biological pathways. Over-represented signatures, based on GO terms (cellular localization, molecular function and biological process) were identified using statistical Fisher's test ($P < 0.05$) and the whole MOE430A gene list as the reference list. The complete, minimum information about a microarray experiment (MIAME)-compliant dataset is available at the public repository ArrayExpress at the EBI (Hinxton, UK) (accession number E-MEXP-1467).

Real-time PCR analysis

Two-step quantitative RT-PCR (qRT-PCR) was employed to validate microarray expression data on a selected list of genes (Table 1). Random-primed RT was carried out with 50 ng of RNA and High-Capacity cDNA Archive Kit (Applied Biosystems, Foster City, CA, USA). Reactions lacking enzyme were carried out in tandem for each RNA sample as negative controls. One-fiftieth of the final RT reaction was used as template in qRT-PCR reactions containing HPLC-purified oligonucleotide primers (Thermo Electron, Ulm, Germany) specific for selected genes (the list of oligonucleotide primer sequences utilized in the present work are shown in Table 1). Primers were designed with Primer3 software (http://frodo.wi.mit.edu/cgi-bin/primer3/primer3_www_slow.cgi) using the following settings:

Table 1 Quantitative RT-PCR: oligonucleotide primer sequences

Gene	RefSeq	Forward	Reverse	Amplicon
Actb	NM_007393	CGTAAAGACCTCTATGCCAACA	CCACCGATCCACACAGAGA	161
Ccl2	NM_011333	CTTCTGGGCCTGCTGTTCA	CCAGCCTACTCATTGGGATCA	127
Ccl7	NM_013654	CCTGGGAAGCTGTTATCTTCA	TTGGCTCCTAGGTTGGTTTC	159
Cx3cl1	NM_009142	CATGTGCGACAAGATGACC	CTTGGACCCATTTCTCCTTC	149
Cxcl16	NM_023158	CCATTCTTTATCAGGTTCCAGT	CTCGTGTCCGAAGGTGTC	200
Egr1	NM_007913	CCTGACCACAGAGTCCTTTT	ATAGGTGATGGGAGGCAAC	103
IL6	NM_031168	GAGGATACCACTCCCAACAGACC	AAGTGCATCATCGTTGTTCATACA	141
Jam2	NM_023844	TGCTGGAGAGTATCGCTGT	CTTCTTTATCCTGGCATCGT	157
Ptgs2	NM_011198	GGTGTGAACAATCAAACAAAATG	TAACATGCTTGGGTCAGTCAAT	160
Vcam1	NM_011693	GAACTGATTATCCAAGTCTCTCCA	CCATGTCTCCTGTCTTTGCTT	157

100–200 bp PCR products, 18–22 mer primers, 60°C melting temperatures. Gene names, accession numbers and forward and reverse primer sequences are listed in Table 1 with the only exception for the *Cxcl1* gene that was analysed by using a Gene Expression Assay (Mm00433859_m1) from Applied Biosystems and the manufacturer's TaqMan® PreAmp Master Mix Kit Protocol. Each primer set produced a single product, as determined by melt-curve analysis. Real-time PCR was carried out on a iCycler Real-Time PCR Detection System (BioRad Richmond, CA, USA) using 25-μl reactions containing iQ SYBR Green Supermix, 150–300 nM forward and reverse primers and 5 μl of cDNA-diluted template. The PCR cycling profile was as follows: 3 min. at 95°C and 40 cycles for 15 sec. at 95°C, 60°C for 1 min. After PCR amplification, melting curve analysis was performed for each reaction.

Each PCR reaction was performed in triplicate on one plate and fluorescence data were recorded using iCycler software (BioRad). Relative expression ratios were calculated by use of Pfaffl equation and Relative Expression Software Tool (http://www.gene-quantification.info). The mRNA expression levels of target genes were normalized to the levels of β-actin gene, which, according to microarray experiments, behaves as a housekeeping gene under the tested conditions.

Endothelial cell adhesion to FGF2-coated plastic dishes

Adhesion of 1G11 cells to FGF2-coated plastic dishes was performed as described [23] with minor modifications. Non-tissue polystyrene culture plastic 35-mm dishes were incubated with 100 mM $NaHCO_3$, pH 9.6 (carbonate buffer) containing 5 μg/ml of FGF2. After 16 hrs of incubation at 4°C, the dishes were washed with cold carbonate buffer and DMEM containing 0.5% FBS. Then, serum-starved 1G11 cells were seeded at 100,000 cells/dish and incubated for 24 hrs in DMEM/0.5% FBS. Cells were dissociated in Trizol for RNA extraction followed by qRT-PCR. The conditioned medium (CM) from FGF2-stimulated cells was collected and stored at −20°C until use. For comparison, confluent cultures of 1G11 cells were treated for 24 hrs with 30 ng/ml of free human recombinant FGF2 whereas untreated cells seeded on tissue culture polystyrene plastic plates were used as negative controls.

Chemotaxis assay

Human monocytes were obtained from buffy coats of healthy blood donors by Ficoll (Lympholite-H, Cederlane Labs, Hornly, Canada) and Percoll (GE Healthcare, Little Chalfont, UK) gradients. Chemotaxis was assayed in 96 well-plates (Neuro Probe, Inc., Gaithersburg, MD, USA) containing a polycarbonate filter with 5-μm pores. Briefly, monocytes were resuspended in RPMI-1640 medium containing 1% serum, and then loaded onto inserts at 5×10^3 cells/50 μl for each well. Thirty microlitres of RPMI-1640 medium containing the chemoattractants at the indicated concentrations were placed in the bottom compartment. After 1.5 hrs of incubation at 37°C with 5% CO_2, non-migrating cells were scraped from the upper surface of the filter. Migrating cells on the lower surface were fixed with methanol, stained with Diff-Quik (Baxter Healthcare, Miami, FL, USA) and their number was determined by counting five microscopic fields per well at ×250 magnification. For inhibitory assays, cells and media were pre-incubated for 30 min. with the indicated concentrations of the pan-chemokine inhibitor M3 before loading onto Transwell inserts (Sigma-Aldrich). Each sample was tested in triplicate.

Matrigel plug angiogenesis assay

Liquid Matrigel (10 mg/ml; 0.5 ml/mouse) was mixed at 4°C with FGF2 (1.0 μg/ml) and injected subcutaneously into the flank of 6-week-old C57BL/6 mice (Charles River, Calco, Italy). Matrigel with PBS alone was used as negative control. Alternatively, 5-week-old 129sv WT and 129sv $PI3K\gamma^{-/-}$ mice [24] were used. On day 7 after implantation, mice were killed and plugs were removed, embedded in Tissue Tec OCT (Sigma-Aldrich), snap-frozen in liquid nitrogen-cooled isopentane and stored at −80°C.

Macrophage depletion

Six-week-old C57BL/6 mice were injected intraperitoneally with clodronate liposomes (Clodro-lip) or PBS liposomes (PBS-lip) every 4 days (initial dose 1.5 mg/20 g mouse, then every fourth day 0.8 mg/20 g mouse) for 4 weeks as described [25]. During the fourth week of treatment, mice were

used for the FGF2-Matrigel assay as described above and killed by cervical dislocation 3 days after the last clodronate liposome injection.

Immunofluorescence analysis

Eight micrometres frozen sections of Matrigel plugs were fixed in ice-cold acetone. After blocking with 10% goat serum in Tris-buffered saline, sections were stained with rat IgG2b monoclonal antibodies raised against mouse CD45, mouse F4/80 or mouse CD11b (all at 1/100 dilution, Serotec, Martinsried/Planegg, Germany), followed by incubation with FITC-conjugated goat anti-rat IgG antibody (1/100 dilution, Santa Cruz, Biotechnology, Santa Cruz, CA, USA). Alternatively, to evaluate microvessel density, sections were incubated with rat IgG2a antimouse CD31 monoclonal antibody followed by incubation with biotinylated mouse anti-rat IgG1/2a antibody (both at 1/100 dilution, BD Pharmingen, San Diego, CA, USA) and Texas red avidin (1/800 dilution, Vector Laboratories, Inc., Burlingame, CA, USA). Nuclei were counterstained by 4′,6-diamidino-2-phenylindole (Sigma-Aldrich). For imaging analysis, CD31 immunostaining was performed on F4/80-pre-stained sections. Images were acquired using an epifluorescence microscope (Zeiss, Inc., Jena, Germany) equipped with an Olympus N547 digital camera (Olympus, Hamburg, Germany) at $\times$200 magnification.

Imaging and statistical analysis

Experimental groups included at least five mice. The Matrigel regions containing the most intense $CD31^+$ areas of neovascularization ('hotspots') were chosen for quantification. Five hotspots per Matrigel section and two sections per Matrigel plug were analysed. The ImagePro Plus analysis system was used to measure $CD31^+$ and $F4/80^+$ areas in each hotspot. Statistical analysis was performed with two-tailed Student's t-test. Differences were considered statistically significant at $P < 0.05$.

Chicken embryo chorioallantoic membrane (CAM) assay

Alginate beads (5 μl) containing the sample under test were placed on top of the CAM of fertilized White Leghorn chicken eggs at day 11 of incubation [26]. After 72 hrs, blood microvessels entering the implants within the focal plane of the CAM were counted *in ovo* at $\times$5 magnification using a STEMI SR stereomicroscope equipped with an objective *f* equal to 100 mm with adapter ring 475070 (Zeiss). Then, the CAMs were cut, fixed with 4% paraformaldehyde and stained May Grünwald-Giemsa to visualize the inflammatory infiltrate. The experiments were repeated at least twice with 7–10 eggs per group.

Results

Transcriptional profiling of FGF2-stimulated murine microvascular endothelial cells reveals a pro-inflammatory signature

To assess the effect of FGF2 on the transcriptional profile of microvascular endothelium, confluent monolayers of mouse lung capillary endothelial 1G11 cells were stimulated for 10 hrs with 30 ng/ml FGF2 in low-serum culture medium. The transcriptional profile was then determined by microarray analysis using Affymetrix MOE4303A genechips (consisting of 22,690 probe sets, corresponding to approximately 15,000 genes) and compared to that of unstimulated cells.

FGF2 treatment exerts a significant impact on the microvascular endothelial cell transcriptome. Indeed, 239 FGF2-modulated genes were identified by combining twofold change filtering with statistical significance analysis. Among these genes, 146 transcripts were up-regulated following FGF2 stimulation whereas 93 genes were down-regulated. Most of the FGF2-modulated transcripts correspond to annotated genes whereas 14 genes were unidentified or hypothetical (a comprehensive list of all the differentially expressed genes is provided in Table 2).

To gather biological information about the FGF2-regulated transcriptional profile, we performed data mining on the web-based database DAVID [22] that provides functional genomic annotations according to GO.

The most over-represented GO terms, based on their statistical significance, were 'extracellular space' (cellular component), 'receptor binding/growth factor activity' (molecular function) and 'blood vessel morphogenesis/angiogenesis' (biological process) (Table 3). Accordingly, data mining on published research literature revealed a clear trend towards the process of new blood vessel formation (Table 4). Indeed, several FGF2-upregulated genes encode for angiogenesis-promoting extracellular factors and cytokines, including *Fgf2* itself, *heparin-binding EGF-like growth factor* (*Hb-egf*), *prolactin family 2, subfamily c, member 2/Proliferin* (*Prl2c2/Plf*), *slit homolog-2* (*Slit2*), *transforming growth factor-b1* (*Tgfb1*) and *Tgfa*, *ephrin-B2* (*EfnB2*), *Drm/gremlin-1*, *Ccl2*, *Cx3cl1*, *Cxcl16*, *platelet-derived growth factor-b* (*Pdgf-b*), *IL-6* and *connective tissue growth factor* (*Ctgf*). Angiogenesis-related genes were also found in the categories of membrane receptors [*anthrax toxin receptor-2* (*Antxr2*), *calcitonin receptor-like receptor* (*Calcrl*), *integrin* α_5 (*Itg5*), *endothelial differentiation sphingolipid G-protein-coupled receptor-1 (Edg1)*, *lymphatic vessel endothelial hyaluronan receptor 1 (Lyve1)*, *prostaglandin E receptor 4 (Ptger4)*, *urokinase-type plasminogen activator receptor* (*Plaur*), *coagulation factor III (F3)*], transcriptional regulators [(*early growth response 1* (*Egr1*), *runt-related transcription factor (Runx) 1* and *2*, *ankyrin repeat domain 1* (*Ankrd1*)], cell adhesion molecules [*CD44 antigen*], proteases and their inhibitors [*matrix metallopeptidase 13* (*Mmp13*), *serpine1*, *serpinb2*, *tissue inhibitor of metalloproteinase 1* (*Timp1*)] (Table 4).

A second enriched biological category within the FGF2-modulated gene list was related to the bone formation process (GO terms 'ossification', 'bone mineralization', 'regulation of bone remodelling') (Table 3), a process in which FGF2 has been shown to play a relevant role [27, 28]. Genes of this functional cluster include master regulators of osteoblast development and function as *Tgfb1* and the transcriptional factor *Runx2*. Other genes related to bone remodelling were the prostaglandin receptor *Ptger4*, the transcriptional factor *Egr2*, the protease *Mmp13* and downstream *TGFb1*/*Runx2* target genes like the bone matrix components *Opn* and *Mgp* (Table 4).

Table 2 FGF2-regulated genes in microvascular 1G11 endothelial cells

FGF2-upregulated genes (fold change > 2; P < 0.05)				
Fold change	***Gene symbol***	***Gene name***	***Unigene ID***	***Affymetrix ID***
21.5	Mmp13	Matrix metallopeptidase 13	Mm.5022	1417256_at
18.5	Ptgs2	Prostaglandin-endoperoxide synthase 2	Mm.292547	1417262_at
14.3				1417263_at
16.4	Sprr1a	Small proline-rich protein 1A	Mm.331191	1449133_at
13.4	Prl2c2	Prolactin family 2, subfamily c, member 2	Mm.88796	1427760_s_at
11.1	Spp1	Secreted phosphoprotein 1	Mm.288474	1449254_at
8.4	Hbegf	Heparin-binding EGF-like growth factor	Mm.289681	1418350_at
7.1				1418349_at
8.1	Ereg	Epiregulin	Mm.4791	1419431_at
7.8	Sgk	Serum/glucocorticoid regulated kinase	Mm.28405	1416041_at
7.7	Hmga2	High mobility group AT-hook 2	Mm.157190	1450780_s_at
7.3				1422851_at
5.8				1450781_at
7.0	Prkg2	Protein kinase, cGMP-dependent, type II	Mm.263002	1435162_at
6.0	1600029D21Rik	RIKEN cDNA 1600029D21 gene	Mm.29959	1423933_a_at
6.0	Cd44	CD44 antigen	Mm.423621	1452483_a_at
4.9				1423760_at
6.0	Errfi1	ERBB receptor feedback inhibitor 1	Mm.318841	1416129_at
2.6				1419816_s_at
5.7	1810011O10Rik	RIKEN cDNA 1810011O10 gene	Mm.25775	1451415_at
5.6	Serpinb2	Serine (or cysteine) peptidase inhibitor, clade B, member 2	Mm.271870	1419082_at
5.5	Egr2	Early growth response 2	Mm.290421	1427683_a_at
4.9				1427682_at
5.0	Ivl	Involucrin	Mm.207365	1422222_at
4.9	Tnfrsf23	Tumour necrosis factor receptor superfamily, member 23	Mm.290780	1422101_at
4.8	Ptger4	Prostaglandin E receptor 4 (subtype EP4)	Mm.18509	1424208_at
4.1				1421073_a_at
4.2	Fosl1	Fos-like antigen 1	Mm.6215	1417487_at
3.2				1417488_at
4.2	Tnfrsf22	Tumour necrosis factor receptor superfamily, member 22	Mm.261384	1422039_at
3.1				1422038_a_at

Continued

Table 2 Continued

FGF2-upregulated genes (fold change > 2; P < 0.05)				
Fold change	***Gene symbol***	***Gene name***	***Unigene ID***	***Affymetrix ID***
2.1				1426095_a_at
4.1	Mgp	Matrix Gla protein	Mm.243085	1448416_at
4.0	Edg1	Endothelial differentiation sphingolipid G-protein-coupled receptor 1	Mm.982	1423571_at
3.8	Hmga1	High mobility group AT-hook 1	Mm.4438	1416184_s_at
3.8	Il6	Interleukin 6	Mm.1019	1450297_at
3.8	Arhgap6	Rho GTPase activating protein 6	Mm.441810	1451867_x_at
2.7				1456333_a_at
2.6				1417704_a_at
3.6	Ier2	Immediate early response 2	Mm.399	1416442_at
3.6	Metrnl	Meteorin, glial cell differentiation regulator-like	Mm.153566	1424356_a_at
3.5	Egr1	Early growth response 1	Mm.181959	1417065_at
3.5	Ccl2	Chemokine (C-C motif) ligand 2	Mm.290320	1420380_at
3.5	Gfpt2	Glutamine fructose-6-phosphate transaminase 2	Mm.24402	1418753_at
3.4	Ccrn4l	CCR4 carbon catabolite repression 4-like (S. Cerevisiae)	Mm.86541	1425837_a_at
3.4	Pvr	Poliovirus receptor	Mm.227506	1450295_s_at
3.3				1423905_at
2.8				1423903_at
2.7				1451160_s_at
3.3	Myc	Myelocytomatosis oncogene	Mm.2444	1424942_a_at
3.2	A030007L17Rik	RIKEN cDNA A030007L17 gene	Mm.294708	1435695_a_at
3.2	Plaur	Plasminogen activator, urokinase receptor	Mm.1359	1452521_a_at
3.2	Dusp6	Dual specificity phosphatase 6	Mm.1791	1415834_at
3.2	Hk2	Hexokinase 2	Mm.255848	1422612_at
3.2	Slc2a1	Solute carrier family 2 (facilitated glucose transporter), member 1	Mm.21002	1426599_a_at
3.1				1426600_at
2.8				1434773_a_at
3.1	Ccl7	Chemokine (C-C motif) ligand 7	Mm.341574	1421228_at
3.1	Serpine1	Serine (or cysteine) peptidase inhibitor, clade E, member 1	Mm.250422	1419149_at
3.1	Gch1	GTP cyclohydrolase 1	Mm.10651	1420499_at
3.1				1429692_s_at
3.1	Vcam1	Vascular cell adhesion molecule 1	Mm.76649	1451314_a_at
2.6				1415989_at
3.1	Mmd	Monocyte to macrophage differentiation associated	Mm.277518	1423489_at

Continued

Table 2 Continued

FGF2-upregulated genes (fold change > 2; P < 0.05)				
Fold change	***Gene symbol***	***Gene name***	***Unigene ID***	***Affymetrix ID***
2.6				1423488_ats
3.1	Pdgfb	Platelet-derived growth factor, B polypeptide	Mm.144089	1450414_at
2.1				1450413_at
3.0	Slc4a7	Solute carrier family 4, sodium bicarbonate cotransporter, member 7	Mm.258893	1438673_at
3.0	Slit2	Slit homolog 2 (Drosophila)	Mm.289739	1424659_at
2.9	Junb	Jun-B oncogene	Mm.1167	1415899_at
2.9	Nr4a1	Nuclear receptor subfamily 4, group A, member 1	Mm.119	1416505_at
2.9	Ell2	Elongation factor RNA polymerase II 2	Mm.21288	1450744_at
2.9	Tnfrsf12a	Tumour necrosis factor receptor superfamily, member 12a	Mm.28518	1418571_at
2.9				1418572_x_at
2.9	Rgs2	Regulator of G-protein signalling 2	Mm.28262	1419248_at
2.6				1419247_at
2.9	Ankrd1	Ankyrin repeat domain 1 (cardiac muscle)	Mm.10279	1420991_at
2.3				1420992_at
2.9	Sox9	SRY-box containing gene 9	Mm.286407	1424950_at
2.1				1451538_at
2.8	F3	Coagulation factor III	Mm.273188	1417408_at
2.8	Grem1	Gremlin 1	Mm.458492	1425357_a_at
2.8	Ifrd1	Interferon-related developmental regulator 1	Mm.168	1416067_at
2.7	Antxr2	Anthrax toxin receptor 2	Mm.24842	1426708_at
2.7	Areg	Amphiregulin	Mm.8039	1421134_at
2.7	Nmt2	N-myristoyltransferase 2	Mm.65021	1423581_at
2.7	Runx1	Runt-related transcription factor 1	Mm.4081	1422864_at
2.4				1422865_at
2.7	Thbs1	Thrombospondin 1	Mm.4159	1450377_at
2.3				1460302_at
2.7	Lrig1	Leucine-rich repeats and immunoglobulin-like domains 1	Mm.245210	1449893_a_at
2.3				1434210_s_at
2.6	Car8	Carbonic anhydrase 8	Mm.119320	1427482_a_at
2.6	Clcf1	cardiotrophin-like cytokine factor 1	Mm.347919	1437270_a_at
2.6	Tnnt2	Troponin T2, cardiac	Mm.247470	1418726_a_at
2.4				1424967_x_at
2.6	Steap1	Six transmembrane epithelial antigen of the prostate 1	Mm.85429	1424938_at

Continued

Table 2 Continued

FGF2-upregulated genes (fold change > 2; P < 0.05)				
Fold change	***Gene symbol***	***Gene name***	***Unigene ID***	***Affymetrix ID***
2.3				1451532_s_at
2.5	Map3k6	Mitogen-activated protein kinase kinase kinase 6	Mm.36640	1449901_a_at
2.5	Fxyd5	FXYD domain-containing ion transport regulator 5	Mm.1870	1418296_at
2.5	Timp1	Tissue inhibitor of metalloproteinase 1	Mm.8245	1460227_at
2.5	Baiap2l1	BAI1-associated protein 2-like 1	Mm.18814	1424951_at
2.5	Adam19	A disintegrin and metallopeptidase domain 19 (meltrin β	Mm.89940	1418403_at
2.4				1418402_at
2.5	1200016E24Rik	RIKEN cDNA 1200016E24 gene	Mm.332931	1435138_s_at
2.3				1453237_s_at
2.5	Ero1l	ERO1-like (S. cerevisiae)	Mm.387108	1419030_at
2.1				1419029_at
2.2				1449324_at
2.4	Tec	Cytoplasmic tyrosine kinase, Dscr28C related (Drosophila)	Mm.319581	1460204_at
2.4	Rhoj	RAS homolog gene family, member J	Mm.27467	1418892_at
2.4	Lyve1	Lymphatic vessel endothelial hyaluronan receptor 1	Mm.396078	1429379_at
2.4	Slc20a2	Solute carrier family 20, member 2	Mm.323901	1434235_at
2.4	Slc25a37	Solute carrier family 25, member 37	Mm.293635	1417750_a_at
2.4	Wisp1	WNT1 inducible signalling pathway protein 1	Mm.10222	1448594_at
2.3				1448593_at
2.4	Cp	Ceruloplasmin	Mm.13787	1455393_at
2.1				1417495_x_at
2.1				1417496_at
2.0				1448734_at
2.4	Tes	Testis-derived transcript	Mm.436548	1460378_a_at
2.1				1424246_a_at
2.3	Calcrl	Calcitonin receptor like	Mm.75467	1425814_a_at
2.3	Dfna5h	Deafness, autosomal dominant 5 homolog (human)	Mm.248361	1421534_at
2.3	Serpina3n	Serine (or cysteine) peptidase inhibitor, clade A, member 3N	Mm.22650	1419100_at
2.3	Tnfaip8	Tumour necrosis factor, -induced protein 8	Mm.27740	1416950_at
2.3	Fgf2	Fibroblast growth factor 2	Mm.457975	1449826_a_at
2.3	Lif	Leukaemia inhibitory factor	Mm.4964	1421207_at
2.3	Plk2	Polo-like kinase 2 (Drosophila)	Mm.380	1427005_at
2.3	Ptpre	Protein tyrosine phosphatase, receptor type, E	Mm.945	1418540_a_at

Continued

Table 2 Continued

FGF2-upregulated genes (fold change > 2; P < 0.05)				
Fold change	***Gene symbol***	***Gene name***	***Unigene ID***	***Affymetrix ID***
2.3	Il1rap	Interleukin 1 receptor accessory protein	Mm.253424	1421844_at
2.3	Ctgf	Connective tissue growth factor	Mm.393058	1416953_at
2.3	Phlda1	Pleckstrin homology-like domain, family A, member 1	Mm.3117	1418835_at
2.3	Oaf	OAF homolog (Drosophila)	Mm.246479	1424086_at
2.3	Jam2	Junction adhesion molecule 2	Mm.41758	1419288_at
2.3				1431416_a_at
2.1				1449408_at
2.3	Slc12a2	Solute carrier family 12, member 2	Mm.399997	1417622_at
2.2				1417623_at
2.3	Hsd17b7	Hydroxysteroid (17-β) dehydrogenase 7	Mm.12882	1417871_at
2.2				1448865_at
2.3	Tnfaip2	Tumour necrosis factor, α-induced protein 2	Mm.255332	1438855_x_at
2.1				1416273_at
2.2	Por	P450 (cytochrome) oxidoreductase	Mm.3863	1416933_at
2.2	Nfil3	Nuclear factor, interleukin 3, regulated	Mm.136604	1418932_at
2.2	Tgfb1	Transforming growth factor, β_1	Mm.248380	1420653_at
2.2	Trib2	Tribbles homolog 2 (Drosophila)	Mm.266679	1426641_at
2.2	Fli1	Friend leukaemia integration 1	Mm.258908	1433512_at
2.2	Etv4	Ets variant gene 4 (E1A enhancer binding protein, E1AF)	Mm.5025	1423232_at
2.2	Btg1	B-cell translocation gene 1, anti-proliferative	Mm.272183	1426083_a_at
2.2	Tgfa	Transforming growth factor α	Mm.137222	1421943_at
2.2	Rai14	Retinoic acid induced 14	Mm.212395	1417401_at
2.2	Osmr	Oncostatin M receptor	Mm.10760	1418674_at
2.1				1418675_at
2.2	Rasa1	RAS p21 protein activator 1	Mm.259653	1426477_at
2.0				1426476_at
2.2	Gprc5b	G protein-coupled receptor, family C, group 5, member B	Mm.103439	1451411_at
2.0				1424613_at
2.1	Hmgcr	3-hydroxy-3-methylglutaryl-Coenzyme A reductase	Mm.316652	1427229_at
2.1	Grwd1	Glutamate-rich WD repeat containing 1	Mm.274847	1455841_s_at
2.1	Lrrc8c	Leucine-rich repeat containing 8 family, member C	Mm.319847	1423614_at
2.1	Chst11	Carbohydrate sulfotransferase 11	Mm.360747	1450509_at
2.1	Fos	FBJ osteosarcoma oncogene	Mm.246513	1423100_at
2.1	Tnfsf9	Tumour necrosis factor (ligand) superfamily, member 9	Mm.41171	1422924_at

Continued

Table 2 Continued

FGF2-downregulated genes (fold change < 2; P < 0.05)				
Fold change	**Gene symbol**	**Gene name**	**Unigene ID**	**Affymetrix ID**
2.1	Runx2	Runt-related transcription factor 2	Mm.391013	1424704_at
2.1	Cyb561	Cytochrome b-561	Mm.149403	1417507_at
2.1	Mpp6	Membrane protein, palmitoylated 6 (MAGUK p55 subfamily member 6)	Mm.41288	1449348_at
2.1	B4galt6	UDP-Gal: βGlcNAc β 1,4-galactosyltransferase, polypeptide 6	Mm.398181	1460329_at
2.1	Spred1	Sprouty protein with EVH-1 domain 1, related sequence	Mm.392726	1423161_s_at
2.1	Efnb2	Ephrin B2	Mm.209813	1449548_at
2.1				1419639_at
2.0				1419638_at
2.1	Enc1	Ectodermal-neural cortex 1	Mm.241073	1450061_at
2.1				1420965_a_at
2.0	Snai1	Snail homolog 1 (Drosophila)	Mm.2093	1448742_at
2.0	Maff	v-maf musculoaponeurotic fibrosarcoma oncogene family, protein F (avian)	Mm.86646	1418936_at
2.0	Rab20	RAB20, member RAS oncogene family	Mm.390014	1438097_at
2.0	Chka	Choline kinase α	Mm.225505	1450264_a_at
2.0	Mthfd2	Methylenetetrahydrofolate dehydrogenase (NAD+ dependent), methenyltetrahydrofolate cyclohydrolase	Mm.443	1419254_at
2.0	Slc20a1	Solute carrier family 20, member 1	Mm.457995	1448568_a_at
2.0	2010002N04Rik	RIKEN cDNA 2010002N04 gene	Mm.273197	1423306_at
2.0	Slco3a1	Solute carrier organic anion transporter family, member 3a1	Mm.425467	1418030_at
2.0	Cx3cl1	Chemokine (C-X3-C motif) ligand 1	Mm.103711	1415803_at
2.0	Flnb	filamin, β	Mm.28095	1426750_at
2.0	1810054D07Rik	RIKEN cDNA 1810054D07 gene	Mm.5540	1440192_at
2.0	Ifi204	Interferon activated gene 204	Mm.442561	1419603_at
2.0	Itga5	Integrin α 5 (fibronectin receptor α)	Mm.16234	1423267_s_at
2.0	Klf10	Kruppel-like factor 10	Mm.4292	1416029_at
2.0	Ier3	Immediate early response 3	Mm.25613	1419647_a_at
2.0	Spred2	Sprouty-related, EVH1 domain containing 2	Mm.266627	1434403_at
2.0	Cyp51	Cytochrome P450, family 51	Mm.140158	1422533_at
2.0	Ier5	Immediate early response 5	Mm.12246	1417612_at
2.0	Eea1	Early endosome antigen 1	Mm.210035	1438045_at
2.0	Cdca7	Cell division cycle associated 7	Mm.270676	1428069_at
2.0	Stc2	Stanniocalcin 2	Mm.32506	1449484_at
2.0	Acsl4	Acyl-CoA synthetase long-chain family member 4	Mm.391337	1433531_at
2.0	Cxcl16	Chemokine (C-X-C motif) ligand 16	Mm.441411	1418718_at
2.0				1449195_s_at

Continued

Table 2 Continued

FGF2-downregulated genes (fold change < 2; P < 0.05)				
Fold change	**Gene symbol**	**Gene name**	**Unigene ID**	**Affymetrix ID**
−5.7	Mettl7a	Methyltransferase like 7A	Mm.220975	1434150_a_at
−5.0				1434151_at
−4.9				1454858_x_at
−4.2				1421184_a_at
−5.1	Akr1c14	Aldo-keto reductase family 1, member C14	Mm.26838	1418979_at
−4.4	Dbp	D site albumin promoter binding protein	Mm.378235	1438211_s_at
−2.7				1418174_at
−3.8	Sord	Sorbitol dehydrogenase	Mm.371580	1426584_a_at
−2.5				1438183_x_at
−3.5	Sesn1	Sestrin 1	Mm.139418	1454699_at
−3.3				1438931_s_at
−3.0				1433711_s_at
−3.3	Sncaip	Synuclein, α interacting protein (synphilin)	Mm.292168	1423499_at
−3.1	---	Transcribed locus	Mm.391736	1455582_at
−3.1	Rab40b	Rab40b, member RAS oncogene family	Mm.281639	1436566_at
−3.1	Angptl7	Angiopoietin-like 7	Mm.388929	1451478_at
−3.3	Tgm2	Transglutaminase 2, C polypeptide	Mm.330731	1455900_x_at
−3.1				1417500_a_at
−3.1				1433428_x_at
−3.1				1437277_x_at
−2.7				1426004_a_at
−3.0	Ptplad2	Protein tyrosine phosphatase-like A domain containing 2	Mm.386788	1450967_at
−3.0	Mapre2	Microtubule-associated protein, RP/EB family, member 2	Mm.132237	1451989_a_at
−3.0	Unc119	Unc-119 homolog (C. elegans)	Mm.284811	1418123_at
−3.0	AW548124	Expressed sequence AW548124	Mm.311974	1454838_s_at
−2.4				1460411_s_at
−2.9	Rasl11b	RAS-like, family 11, member B	Mm.293316	1423854_a_at
−2.9	D0H4S114	DNA segment, human D4S114	Mm.407415	1436736_x_at
−2.8				1450839_at
−2.8	Bnc1	Basonuclin 1	Mm.243802	1424890_at
−2.8	Sfrp2	Secreted frizzled-related protein 2	Mm.19155	1448201_at
−2.8	Ogn	Osteoglycin	Mm.4258	1419663_at

Continued

Table 2 Continued

FGF2-downregulated genes (fold change < 2; P < 0.05)				
Fold change	**Gene symbol**	**Gene name**	**Unigene ID**	**Affymetrix ID**
−2.5				1419662_at
−2.7	Antxr1	Anthrax toxin receptor 1	Mm.232525	1451446_at
−2.7	Trp53inp1	Transformation-related protein 53 inducible nuclear protein 1	Mm.393018	1416926_at
−2.3				1416927_at
−2.6	Slc1a6	Solute carrier family 1 (high-affinity aspartate/glutamate transporter), member 6	Mm.6257	1418933_at
−2.6	Fhl1	Four and a half LIM domains 1	Mm.3126	1417872_at
−2.6	Pkia	Protein kinase inhibitor, α	Mm.3193	1420858_at
−2.6				1420859_at
−2.6	Ddit4l	DNA-damage-inducible transcript 4-like	Mm.250841	1451751_at
−2.4				1439332_at
−2.6	Vldlr	Very low density lipoprotein receptor	Mm.4141	1417900_a_at
−2.3				1434465_x_at
−2.6	Fzd2	Frizzled homolog 2 (Drosophila)	Mm.36416	1418534_at
−2.1				1418532_at
−2.1				1418533_s_at
−2.5	Pdlim3	PDZ and LIM domain 3	Mm.282900	1449178_at
−2.5	Dhrs3	Dehydrogenase/reductase (SDR family) member 3	Mm.14063	1448390_a_at
−2.5	Ephx2	Epoxide hydrolase 2, cytoplasmic	Mm.15295	1448499_a_at
−2.5	Gab1	Growth factor receptor bound protein 2-associated protein 1	Mm.277409	1417694_at
−2.3				1417693_a_at
−2.4	Zfp521	Zinc finger protein 521	Mm.40325	1451332_at
−2.4	Sspn	Sarcospan	Mm.49689	1417644_at
−2.4	Oplah	5-oxoprolinase (ATP-hydrolysing)	Mm.322738	1424359_at
−2.4	Mcam	Melanoma cell adhesion molecule	Mm.275003	1416357_a_at
−2.4	Figf	C-Fos induced growth factor	Mm.297978	1438954_x_at
2.3				1438953_at
−2.3	Npr3	Natriuretic peptide receptor 3	Mm.25259	1435184_at
−2.3	Mmp11	Matrix metallopeptidase 11	Mm.4561	1417234_at
−2.3	Tek	Endothelial-specific receptor tyrosine kinase	Mm.14313	1418788_at
−2.3	Wdr6	WD repeat domain 6	Mm.335454	1415770_at
−2.3				1455940_x_at
−2.2	Adamts5	A disintegrin-like and metallopeptidase (reprolysin type) with thrombospondin type 1 motif, 5 (aggrecanase-2)	Mm.112933	1422561_at
−2.2	Pdgfra	Platelet-derived growth factor receptor, α polypeptide	Mm.221403	1421917_at
−2.2	Appl2	Adaptor protein, phosphotyrosine interaction, PH domain and leucine zipper containing 2	Mm.282985	1426743_at

Continued

Table 2 Continued

FGF2-downregulated genes (fold change < 2; P < 0.05)				
Fold change	**Gene symbol**	**Gene name**	**Unigene ID**	**Affymetrix ID**
−2.2	Stard10	START domain containing 10	Mm.28896	1448956_at
−2.2	Fgf18	Fibroblast growth factor 18	Mm.339812	1449545_at
−2.2	Apbb1	Amyloid , (A4) precursor protein-binding, family B, member 1	Mm.38469	1423893_x_at
−2.2	Palm	Paralemmin	Mm.34650	1423967_at
−2.2	Slc25a23	Solute carrier family 25 (mitochondrial carrier; phosphate carrier), member 23	Mm.23720	1419045_at
−2.2	Igf1	Insulin-like growth factor 1	Mm.268521	1437401_at
−2.2	Serpinb9	Serine (or cysteine) peptidase inhibitor, clade B, member 9	Mm.272569	1422601_at
−2.2	Gamt	Guanidinoacetate methyltransferase	Mm.7329	1422558_at
−2.2	Klhl13	Kelch-like 13 (Drosophila)	Mm.224306	1448269_a_at
−2.0				1416242_at
−2.2	Acaa2	Acetyl-Coenzyme A acyltransferase 2 (mitochondrial 3-oxoacyl-Coenzyme A thiolase)	Mm.245724	1455061_a_at
−2.0				1428146_s_at
−2.1	Slc39a8	Solute carrier family 39 (metal ion transporter), member 8	Mm.30239	1416832_at
−2.1	Dzip1	DAZ interacting protein 1	Mm.87456	1452792_at
−2.1	Aldh1a7	Aldehyde dehydrogenase family 1, subfamily A7	Mm.14609	1418601_at
−2.1	2310002J21Rik	RIKEN cDNA 2310002J21 gene	Mm.375091	1456393_at
−2.1	Pmp22	Peripheral myelin protein	Mm.1237	1417133_at
−2.1	Ifit3	Interferon-induced protein with tetratricopeptide repeats 3	Mm.426079	1449025_at
−2.1	Tsc22d3	TSC22 domain family 3	Mm.22216	1425281_a_at
−2.1	6720475J19Rik	RIKEN cDNA 6720475J19 gene	Mm.273536	1423072_at
−2.1	Rtn1	Reticulon 1	Mm.221275	1429761_at
−2.1	Pdcd4	Programmed cell death 4	Mm.1605	1418840_at
−2.1	Cables1	Cdk5 and Abl enzyme substrate 1	Mm.40717	1422477_at
−2.1	Reck	Reversion-inducing cysteine-rich protein with kazal motifs	Mm.331573	1450784_at
−2.1	Gsta3	Glutathione S-transferase, α3	Mm.394593	1423436_at
−2.1	Myl7	Myosin, light polypeptide 7, regulatory	Mm.46514	1449071_at
−2.1	Cd200	Cd200 antigen	Mm.245851	1448788_at
−2.1	1200015N20Rik	RIKEN cDNA 1200015N20 gene	Mm.19825	1448557_at
−2.1	Ptprd	Protein tyrosine phosphatase, receptor type, D	Mm.184021	1429052_at
−2.1	Dcxr	Dicarbonyl L-xylulose reductase	Mm.231091	1419456_at
−2.1	Gadd45b	Growth arrest and DNA-damage-inducible 45 β	Mm.1360	1450971_at
−2.1				1449773_s_at
−2.0	Atp6v0e2	ATPase, H+ transporting, lysosomal V0 subunit E2	Mm.458098	1448211_at
−2.0	4930570C03Rik	RIKEN cDNA 4930570C03 gene	Mm.28955	1450410_a_at

Continued

Table 2 Continued

FGF2-downregulated genes (fold change < 2; P < 0.05)				
Fold change	**Gene symbol**	**Gene name**	**Unigene ID**	**Affymetrix ID**
−2.0	Sorbs1	Sorbin and SH3 domain containing 1	Mm.210815	1436737_a_at
−2.0	Add3	Adducin 3 (γ)	Mm.426080	1423298_at
−2.0	Hadh	Hydroxyacyl-Coenzyme A dehydrogenase	Mm.260164	1460184_at
−2.0	Oprl1	Opioid receptor-like 1	Mm.285075	1450486_a_at
−2.0	Armcx3	Armadillo repeat containing, X-linked 3	Mm.67949	1460359_at
−2.0	Klhl24	Kelch-like 24 (Drosophila)	Mm.392914	1451793_at
−2.0	---	Transcribed locus	Mm.275414	1454967_at
−2.0	Zfp810	Zinc finger protein 810	Mm.306038	1451566_at
−2.0	Pdk2	Pyruvate dehydrogenase kinase, isoenzyme 2	Mm.29768	1448825_at
−2.0	Abhd14b	Abhydrolase domain containing 14b	Mm.335427	1451326_at
−2.0	Mxd4	Max dimerization protein 4	Mm.391777	1434378_a_at
−2.0	Marcksl1	MARCKS-like 1	Mm.424974	1437226_x_at
−2.0	Bckdha	Branched chain ketoacid dehydrogenase E1, α polypeptide	Mm.25848	1416647_at
−2.0	Stk17b	Serine/threonine kinase 17b (apoptosis-inducing)	Mm.25559	1450997_at
−2.0	Spag5	Sperm associated antigen 5	Mm.24250	1433893_s_at
−2.0	Aldoc	Aldolase 3, C isoform	Mm.7729	1451461_a_at
−2.0	Tuft1	Tuftelin 1	Mm.10214	1416689_at
−2.0	Tmem9	Transmembrane protein 9	Mm.41773	1419557_a_at
−2.0	Calml4	Calmodulin-like 4	Mm.440576	1424713_at

The fold change, the official gene symbol and name, the Unigene cluster and the Affymetrix probe set ID number are shown. Note that various genes are interrogated by more than one probe set in the Affymetrix MOE430A genechip.

Interestingly, a third prominent group of FGF2-induced genes was related to the inflammatory response (Table 3). As shown in Table 4, FGF2 up-regulates the expression of a number of chemokines involved in the recruitment of different inflammatory cells such as monocytes/macrophages (*Ccl2*, *Ccl7*, *Cx3cl1*, *Opn*), neutrophils (*Cxcl1*), NK cells (*Cx3cl1*) and T lymphocytes (*Cxcl16*, *Cx3cl1*). Also, FGF2-induced genes include inflammatory cytokines [*IL-6*, *leukaemia inhibitory factor* (*Lif*), *Opn*] and cytokine receptors [*oncostatin M receptor* (*Osmr*), *tumour necrosis factor receptor superfamily member 12a* (*Tnfrsf12a*)/*Tweak*-receptor, interleukin *1 receptor accessory protein* (*IL1rap*)], cell adhesion molecules related to leucocyte recruitment and transendothelial migration [*vascular cell adhesion molecule 1* (*Vcam1*), *junctional adhesion molecule 2* (*JAM2*)], as well as key inflammatory mediators like the cyclooxygenase *Ptgs2/Cox-2* and the prostaglandin E_2 receptor *Ptger4*.

It must be pointed out that, given the tight interplay among angiogenesis, bone formation and inflammation, the role exerted by various genes mentioned above (*e.g. Opn*) is not limited to a single biological process (Table 4).

Real-time PCR analysis of FGF2 up-regulated genes

The qRT-PCR was used to confirm the up-regulation of a number of selected inflammation-related genes (*IL-6*, *Ccl2*, *Ccl7*, *Cx3cl1*, *Cxcl1*, *Cxcl16*, *Egr1*, *Jam2*, *Ptgs2/ Cox-2*, *Vcam1*) in FGF2-treated endothelial 1G11 cells. Time-course analysis demonstrated the up-regulation of all the genes examined (Fig. 1), showing an early up-regulation for most of them (1 hr after treatment), thus indicating that the induction of a pro-inflammatory signature represents an early event in FGF2-driven endothelial cell activation. Also, dose–response experiments showed that the selected genes *Ccl2*, *Ccl7* and *Ptgs2*/*Cox-2* were all significantly up-regulated in 1G11 cells when tested at FGF2 concentrations ranging from 1.0 to 30 ng/ml. Moreover, qRT-PCR analysis confirmed the up-regulation of the inflammation-related genes *Ccl2*, *Ccl7*, *Cx3cl1* and *Ptgs2*/*Cox-2* in FGF2-stimulated murine brain microvascular endothelial 10027 cells [29], supporting the notion that the induction of a pro-inflammatory signature represents a general feature of the FGF2-mediated response in endothelium.

FGF2 induces inflammatory cell recruitment in the areas of neovascularization

The above results led us to investigate the presence of FGF2-triggered inflammatory cues in two different *in vivo* models of angiogenesis, the chick embryo CAM assay and the murine Matrigel plug assay.

As shown in Fig. 2, an alginate pellet containing FGF2 triggered a potent angiogenic response when applied on the top of the chick embryo CAM. May Grünwald-Giemsa staining of the FGF2-treated CAMs revealed the presence of an inflammatory cell infiltrate in the stroma among the newly formed blood vessels (Fig. 2). However, the lack of specific antibodies and the early stage of development of the chick embryos did not allow a characterization of the inflammatory cells infiltrating the CAM. Next, the anti-inflammatory drugs hydrocortisone and ketoprofen were used to assess the overall impact of the inflammatory response on FGF2-induced angiogenesis in the CAM assay. As shown in Fig. 2, both drugs were able to inhibit the angiogenic response triggered by FGF2, thus implicating inflammatory cells/mediators in FGF2-dependent neovascularization.

In a second set of experiments, FGF2-embedded Matrigel plugs were implanted subcutaneously in mice and examined hystologically at day 7 after implantation (Fig. 3). Haematoxylin/eosin staining revealed the presence of numerous blood vessels and of an abundant cellular infiltrate in FGF2-embedded pellets when compared to PBS-embedded control implants. Immunofluorescence analysis confirmed the presence of a potent neovascular response in FGF2-embedded plugs, as shown by the presence of numerous $CD31^+$ endothelial cells, which was accompanied by a consistent $CD45^+$ leucocyte infiltrate. The characterization of the leucocyte subsets revealed that the inflammatory cell infiltrate consists mainly of $CD11b^+$ monocytes and $F4/80^+$ macrophages. Only rare $Gr\text{-}1^+$ neutrophils and $CD8^+$ or $CD4^+$ T-lymphocytes and no $CD19^+$ B-lymphocytes, $NK1.1^+$ natural killer or $CD11c^+$ dendritic cells were instead detectable (Fig. 3 and Table 5). A time-course analysis of the cellular populations infiltrating the FGF2-embedded Matrigel plugs revealed that monocytes/macrophages are already detectable within the plug at day 2 after implantation whereas a significant $CD31^+$ neovascular response becomes evident on day 4 (data not shown). Thus, macrophage recruitment precedes neovascularization in FGF2-driven angiogenesis.

Impairment of macrophage recruitment reduces FGF2-induced angiogenesis

The above observations support the notion that inflammatory cells are relevant to FGF2-dependent neovascularization. To further investigate this hypothesis, we evaluated the capacity of FGF2 to trigger an angiogenic response in the Matrigel plug assay under conditions that impair the recruitment of inflammatory cells.

Proper migration of leucocytes to chemotactic agonists in inflammatory sites is dependent on PI3Kγ activity [24]. To investigate the potential role of infiltrating inflammatory cells in the modulation of FGF2-dependent angiogenesis, FGF2-embedded Matrigel plugs were implanted subcutaneously in PI3K$\gamma^{-/-}$ mice and examined by immunostaining at day 7 after implantation. Computerized image analysis of the immunofluorescence signals demonstrated a significant reduction of the $F4/80^+$ cell infiltrate (–60%) and, importantly, of $CD31^+$ neovessels (–40%) in PI3K$\gamma^{-/-}$ mice when compared to wild-type control animals (Fig. 4).

In a second set of experiments, FGF2-induced angiogenesis was evaluated after macrophage depletion following intraperitoneal pre-treatment with clodronate liposomes (Clodro-lip) [30]. Again, immunofluorescence analysis demonstrated a 72% reduction of the $F4/80^+$ macrophage infiltrate and a 40% decrease of the $CD31^+$ areas of neovascularization in FGF2-embedded Matrigel plugs implanted in Clodro-lip-treated animals when compared to control animals injected with PBS-containing liposomes (PBS-lip)

Table 3 Over-represented GO terms for FGF2-upregulated genes in murine microvascular 1G11 cells

GO term	Number of genes	%	Statistical significance
Molecular function			
Receptor binding	34	12.1	1.0E-07
Growth factor activity	18	6.4	1.1E-07
Cytokine activity	19	6.8	2.5E-06
Cellular component			
Extracellular space	69	24.6	2.5E-04
Extracellular region	71	25.4	5.8E-04
Basolateral plasma membrane	6	2.1	6.0E-03
Extracellular matrix	10	3.6	5.2E-02
Biological process			
Blood vessel morphogenesis	19	6.8	2.2E-09
Angiogenesis	16	5.7	4.5E-08
Ossification	13	4.6	2.0E-07
Bone mineralization	8	2.9	3.8E-05
Regulation of bone remodelling	7	2.5	2.7E-05
Inflammatory response	12	4.3	4.4E-04

FGF2-upregulated genes (see Table 2 for the detailed list of these genes) were classified in terms of their associated GO molecular functions, cellular components and biological processes. The most over-represented GO terms, the number and percentage of genes belonging to each category, and the statistical significance are shown.

Table 4 FGF2-upregulated genes in murine microvascular 1G11 endothelial cells related to angiogenesis, bone formation, and inflammation

Growth factors, cytokines and chemokines	*Symbol*	*Biological Process*	*Fold change*
Chemokine (C-C motif) ligand 7	Ccl7	I	3.1
Chemokine (C-X3-C motif) ligand 1	Cx3cl1	A/I	2.0
Chemokine (C-X-C motif) ligand 1	Cxcl1	A/I	2.0
Chemokine (C-X-C motif) ligand 16	Cxcl16	A/I	2.0
Connective tissue growth factor	Ctgf	A/B	2.3
Ephrin B2	Efnb2	A/B	2.1
Fibroblast growth factor 2	Fgf2	A/B/I	2.3
Gremlin 1	Grem1	A	3.1
Heparin-binding EGF-like growth factor	Hbegf	A	8.4
Interleukin 6	Il6	A/B/I	3.8
Leukemia inhibitory factor	Lif	B/I	2.3
Platelet-derived growth factor, B polypeptide	Pdgfb	A	3.2
Prolactin family 2, subfamily c, member 2/Proliferin	Prl2c2/Pfl	A	13.5
Secreted phosphoprotein 1/osteopontin	Spp1/Opn	A/B/I	12.2
Slit homolog 2 (Drosophila)	Slit2	A/I	3.0
Thrombospondin 1	Thbs1	A/B/I	2.7
Transforming growth factor α	Tgfa	A	2.2
Transforming growth factor, β_1	Tgfb1	A/B/I	2.2
Tumor necrosis factor, α-induced protein 2	Tnfaip2	A	2.3
Membrane receptors and adhesion molecules	***Symbol***	***Biological Process***	***Fold change***
Anthrax toxin receptor 2	Antxr2	A	2.7
Calcitonin receptor-like	Calcrl	A/B	2.3
CD44 antigen	Cd44	A/I	6.1
Coagulation factor III	F3/Tf	A/I	2.9
Endothelial differentiation sphingolipid G-protein-coupled receptor 1	Edg1	A	4.1
Integrin α_5 (fibronectin receptor α)	Itga5	A	2.0
Interleukin 1 receptor accessory protein	Il1rap	I	2.3
Junction adhesion molecule 2	Jam2	I	2.3
Lymphatic vessel endothelial hyaluronan receptor 1	Lyve1	A	2.4
Oncostatin M receptor	Osmr	A/B/I	2.2
Plasminogen activator, urokinase receptor	Plaur	A/B/I	3.2
Prostaglandin E receptor 4 (subtype EP4)	Ptger4	A/B/I	4.9
Tumor necrosis factor receptor superfamily, member 12a	Tnfrsf12a	A/B/I	2.9
Vascular cell adhesion molecule 1	Vcam1	I	3.1

Table 4 Continued

Transcriptional regulators	*Symbol*	*Biological Process*	*Fold change*
Early growth response 1	Egr1	A	3.4
Early growth response 2	Egr2	B	5.6
Runt-related transcription factor 1	Runx1	A/B	2.8
Runt-related transcription factor 2	Runx2	A/B	2.1
Ankyrin repeat domain 1 (cardiac muscle)	Ankrd1	A	3.6
Others	*Symbol*	*Biological Process*	*Fold change*
Matrix Gla protein	Mgp	B	4.1
Matrix metallopeptidase 13	Mmp13	A/B	22.1
Prostaglandin-endoperoxide synthase 2	Ptgs2/Cox-2	A/B/I	18.5
Serine (or cysteine) peptidase inhibitor, clade E, member 1	Serpine1	A/I	3.0
Serine (or cysteine) peptidase inhibitor, clade B, member 2	Serpinb2	A	5.6
Tissue inhibitor of metalloproteinase 1	Timp1	A/I	2.5

Selected FGF2-upregulated genes (fold change > 2, $P < 0.05$, see Table 2) were classified in terms of their association with angiogenesis (A), bone formation (B) and inflammation (I) processes, according to the GO database and bibliographic searching.

Table 5 Immunoistochemical characterization of the inflammatory infiltrate in FGF2-Matrigel plugs

Treatment	CD31$^+$	CD45$^+$	CD11b$^+$	F4/80$^+$	GR-1$^+$	CD4$^+$	CD8$^+$
PBS	1074 ± 748	7682 ± 3220	7002 ± 601	2316 ± 186	61 ± 63	0	0
FGF2	12,228 ± 2024	37,467 ± 5900	13,469 ± 2372	17,401 ± 7187	82 ± 115	154 ± 169	654 ± 834

Eight μm frozen sections of Matrigel plugs containing PBS or FGF2 (five plugs per group) were immunostained for the indicated antigens. Then, the corresponding immunoreactive areas were analysed in five microscopic fields per Matrigel section (two sections per Matrigel plug) using the ImagePro Plus software. Analysis was performed on plugs on day 7 after implantation. Data (mean ± SD) are expressed as μm^2 of immunoreactive area per microscopic field (0.38 mm^2).

(Fig. 4). Taken together, these results point to a role for pro-inflammatory macrophages in FGF2-induced angiogenesis *in vivo*.

The conditioned medium from FGF2-stimulated microvascular cells is chemotactic for monocytes and promotes chemokine-dependent angiogenesis *in vivo*

Gene expression data indicate that FGF2 up-regulates the production of various chemokines that may serve to recruit monocytes in the neovascularized areas. To test this hypothesis, we evaluated the ability of the CM from FGF2-stimulated microvascular 1G11 cells to induce monocyte chemotaxis *in vitro*. To avoid the possibility that exogenously added FGF2 may interfere with the biological activity of the CM from FGF2-treated cells, 1G11 cells were seeded on FGF2 immobilized to plastic dishes where it retains a full biological activity [31]. Following a 24-hr stimulation, cells extracts and CM were analysed for gene expression and monocyte chemotactic activity, respectively. The concentration of human FGF2 in the CM was typically lower than 1.0 ng/ml, as assessed by ELISA. As controls, 1G11 cells cultured for 24 hrs on non-coated dishes or stimulated with soluble FGF2 (30 ng/ml) were analysed in parallel. As shown in Fig. 5, both immobilized and free FGF2 induced the up-regulation of selected chemotactic factors, thus confirming the ability of substratum-bound FGF2 to activate endothelial cells.

On this basis, the CM from control and FGF2-stimulated 1G11 cells were tested in a Boyden chamber assay for the capacity to induce a chemotactic response in freshly isolated human monocytes (Fig. 6A). The CM from FGF2-stimulated 1G11 cells exerted a dose-dependent chemotactic response whereas the CM from control cells was ineffective. Importantly, the chemotactic

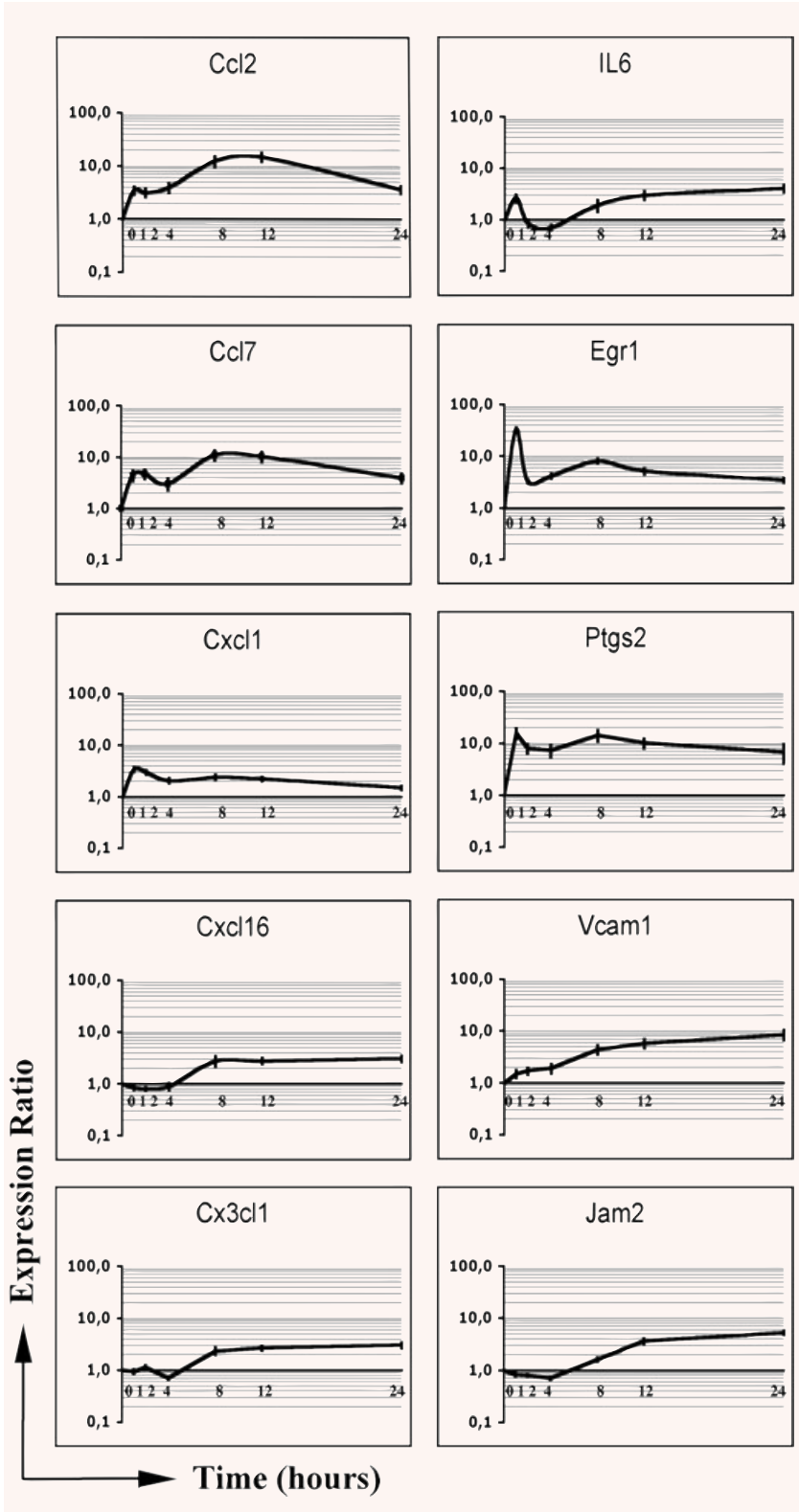

Fig. 1 qRT-PCR time course analysis of selected inflammation-related genes in FGF2-stimulated endothelial cells. Serum starved 1G11 endothelial cells were stimulated with 30 ng/ml of FGF2 for 0, 1, 2, 4, 8, 12 and 24 hrs. Total RNA from each time-point was reverse transcribed to cDNA and analysed by qRT-PCR. Data (mean values ± SD, $n = 3$) represent the expression ratio of each target gene relative to the untreated control. Expression levels were normalized to β-actin gene.

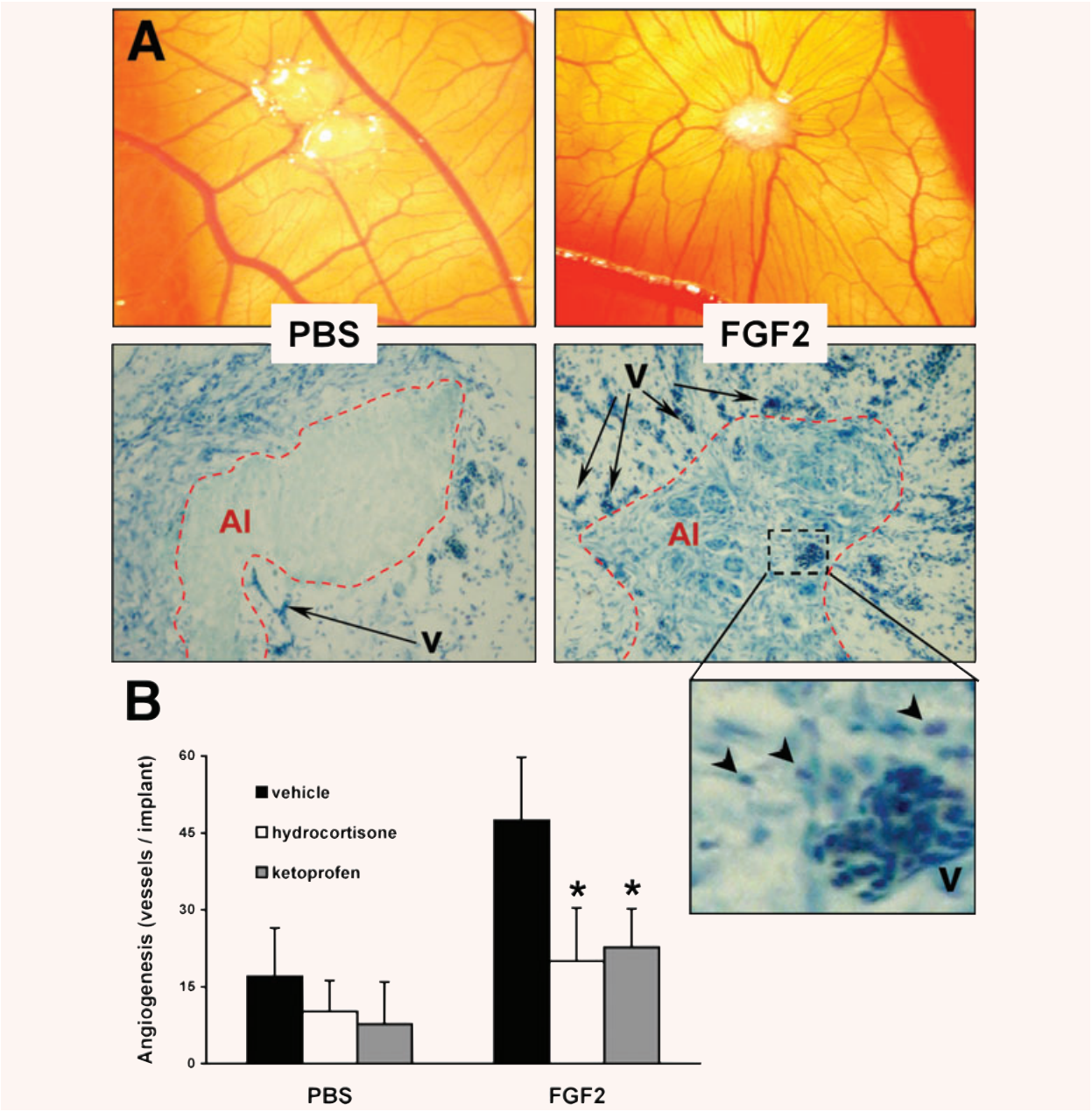

Fig. 2 FGF2 induces angiogenic and inflammatory responses in the chick embryo CAM assay. (**A**) Alginate beads containing vehicle (PBS) or 150 ng of FGF2 (FGF2) were implanted on top of chick embryo CAMs at day 11 of development. After 3 days, CAMs were assessed for new vessel formation (upper panels) using a stereomicroscope (original magnification, ×5) and for inflammatory cell infiltration (lower panels) by May Grünwald-Giemsa staining of paraffin-embedded sections (original magnification, ×40). Note the strong presence of inflammatory cells (*arrowheads*) in the areas of FGF2-induced neovascularization, as shown in the enlarged lower right panel. Alginate implant (AI, dotted line), vessels (v). **(B)** Alginate implants containing vehicle or 150 ng of FGF2 were assessed for their angiogenic capacity in the absence or presence of 50 μg of hydrocortisone or 50 μg of ketoprofen. Data (7–10 eggs per group) represent the number of vessels converging towards the alginate implant and are expressed as mean ± SD. *, statistically different from the 'FGF2 plus vehicle' group, $P < 0.05$.

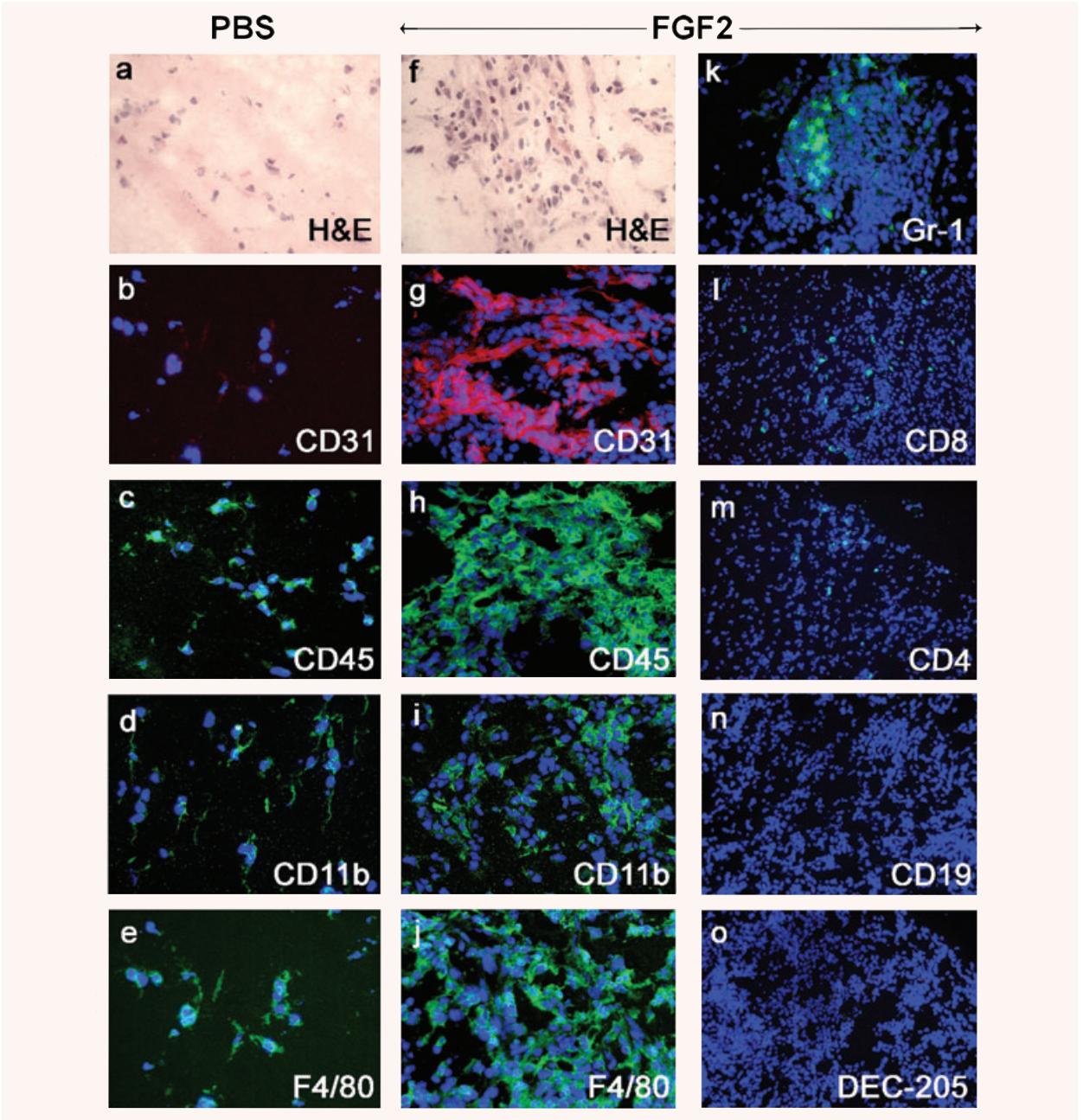

Fig. 3 Inflammatory cells infiltrate the areas of FGF2-induced neovascularization in Matrigel plugs. Matrigel pellets containing PBS or 150 ng of FGF2 were implanted subcutaneously in mice and examined at day 7 by haematoxylin and eosin staining and immunofluorescence analysis with antibodies specific to the indicated antigens. Note the presence in the implanted FGF2-Matrigel plugs of numerous $CD31^+$ endothelial cells and of CD45+ infiltrating leucocytes, mainly consisting of $CD11b^+$ monocytes and $F4/80^+$ macrophages. Only scarce $Gr\text{-}1^+$ neutrophils, $CD8^+$ and $CD4^+$ T-lymphocytes and no $CD19^+$ B-lymphocytes, $NK1.1^+$ natural killer or $CD11c^+$ dendritic cells are instead detectable. Nuclei are shown by DAPI counterstaining. Original magnification: a–j, ×200; k–o, ×100.

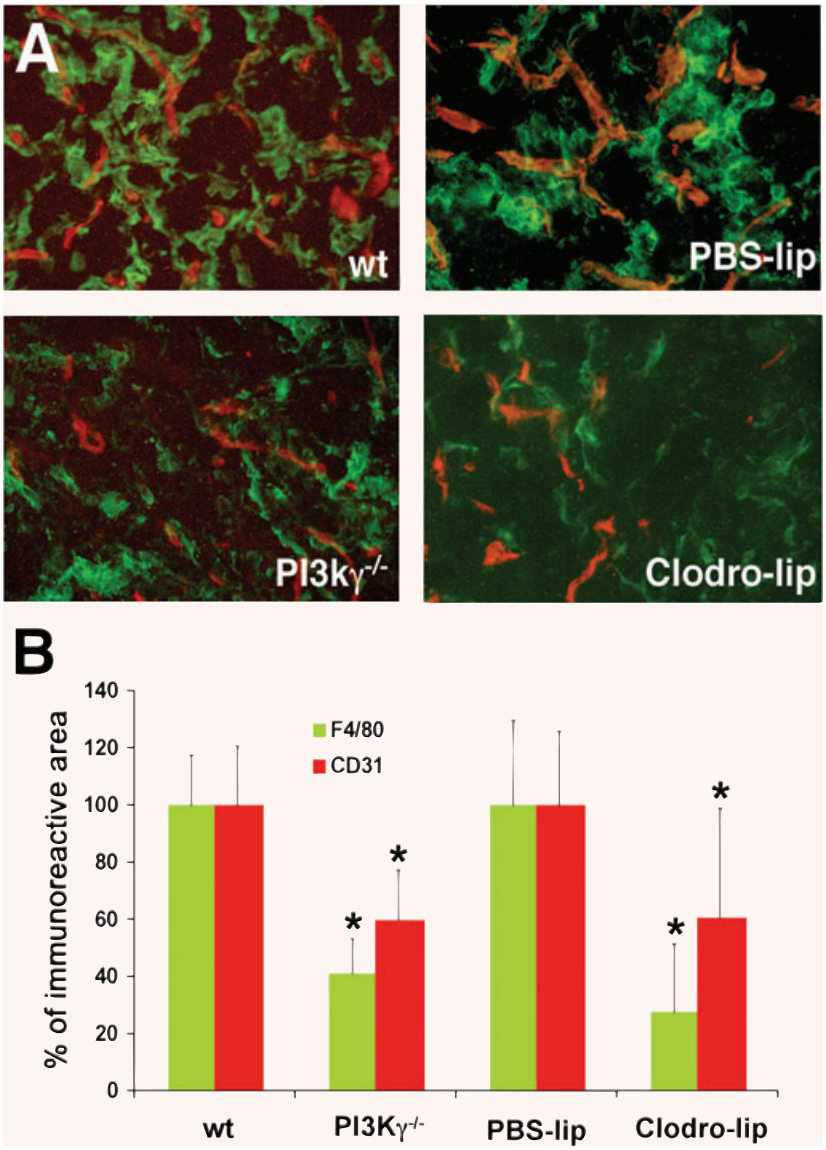

Fig. 4 Defective macrophage recruitment impairs FGF2-induced angiogenesis. **(A)** Immunohistochemical analysis of FGF2-Matrigel pellets from wild-type (wt) or PI3Kγ$^{-/-}$ SV129 mice and from C57Bl/6 mice that underwent PBS-lips or Clodro-lips pretreatment. Matrigel sections were double-stained with anti-CD31 (red) and anti-F4/80 (green) monoclonal antibodies. Original magnification, ×200. **(B)** Quantitative analysis of infiltrating CD31^{+} endothelial cells and F4/80^{+} macrophages in FGF2-Matrigel plugs on day 7 after implantation. Data (mean ± SD) represent the percentage of CD31^{+} (red bars) or F4/80^{+} (green bars) immunopositive areas of Matrigel sections from PI3Kγ$^{-/-}$ or Clodro-lip-treated mice relative to their respective wt and PBS-lip-treated controls. *, $P < 0.05$.

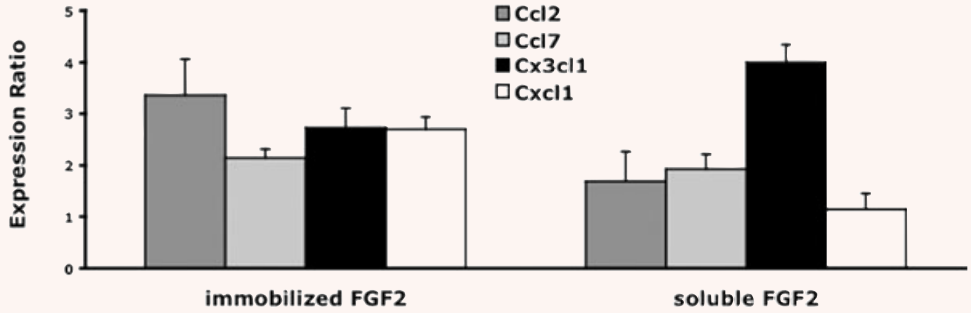

Fig. 5 qRT-PCR analysis of selected chemokines in endothelial cells stimulated by immobilized or soluble FGF2. Microvascular 1G11 cells were incubated for 24 hrs on FGF2-coated dishes (immobilized FGF2) or stimulated for 24 hrs with 30 ng/ml of FGF2 (soluble FGF2) onto non-coated dishes. Total RNA was reverse transcribed to cDNA and analysed by real-time PCR. Data are presented as the expression ratio of each target gene relative to an untreated control. Expression levels were normalized to β-actin gene. The bars show mean values ± SD ($n = 3$).

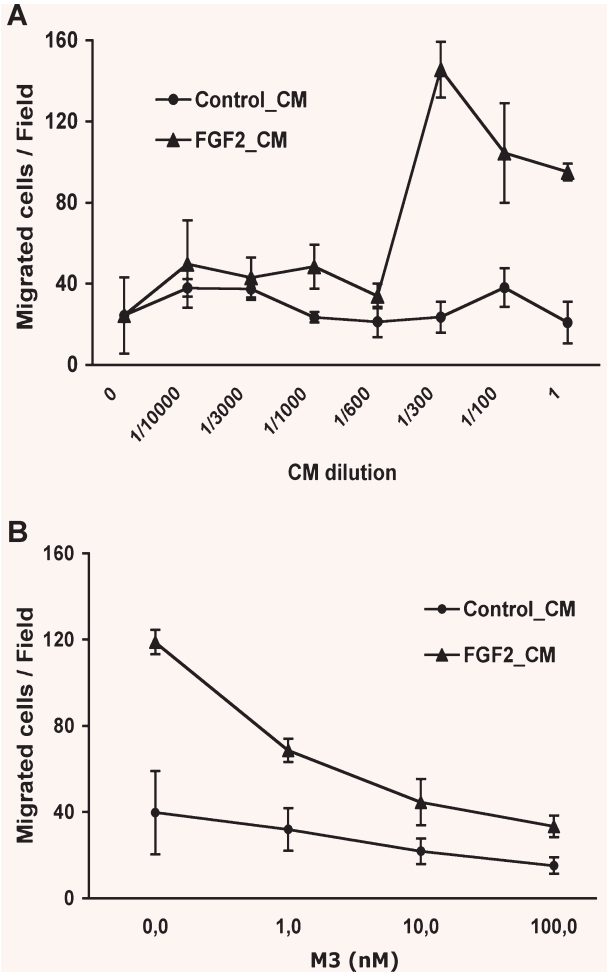

Fig. 6 The conditioned medium (CM) from FGF2-stimulated microvascular endothelial cells is chemotactic to monocytes. **(A)** The migration of human monocytes towards different dilutions of the CM from non-stimulated (Control_CM) and FGF2-stimulated (FGF2_CM) 1G11 endothelial cells was quantified as described in '*Materials and methods*'. Data are expressed as the mean number of migrated cells per field. **(B)** Inhibition of the chemotactic response of 1G11 endothelial cells towards FGF2-CM by different concentrations of the pan-chemokine inhibitor M3. Chemotaxis was tested at the dose of FGF2_CM that induced the maximal chemotactic responses (1/300 dilution) and compared to the equivalent dilution of Control_CM. Data are expressed as the number of migrated cells per field.

response was inhibited in a dose-dependent manner when the CM from FGF2-stimulated 1G11 cells was pre-incubated with the pan-chemokine inhibitor M3 (Fig. 6B), a murine gammaherpesvirus 68 protein antagonist for human and mouse CC, CXC and CX3C chemokines [19]. At variance, M3 did not affect the capacity of FGF2 to trigger *in vitro* endothelial cell proliferation and sprouting (data not shown). Taken together, these observations indicate that FGF2-activated endothelium expresses and secretes biologically active chemokine(s) that represent a chemotactic stimulus for human monocytes.

Next, the CM from FGF2-stimulated microvascular 1G11 cells was investigated for the capacity to induce neovascularization *in vivo* in the chick embryo CAM assay. As shown in Fig. 7A, the CM from FGF2-stimulated endothelial cells exerted a potent angiogenic response that was significantly reduced in the presence of the pan-chemokine inhibitor M3. Accordingly, the intense cellular infiltrate observed in the areas of neovascularization induced by the CM from FGF2-stimulated cells was almost abolished in the presence of M3 (Fig. 7B). In keeping with these observations, the pan-chemokine inhibitor M3 induced a significant inhibitory effect on neovascularization induced by recombinant FGF2, without affecting the basal levels of vascularization of the CAM (Fig. 8). Taken together, these findings demonstrate a relevant role for pro-inflammatory chemokines in FGF2-driven angiogenesis.

Discussion

Scattered experimental evidence pointed to a role for inflammatory mediators and leucocytes in mediating the neovascularization process triggered by the angiogenic growth factor FGF2 [10, 13, 15–17, 32]. In the present study, transcriptome analysis demonstrates that FGF2 activates a complex pro-inflammatory signature in murine microvascular endothelial cells. Accordingly, we provide evidence that FGF2-induced chemokines and infiltrating monocytes/macrophages are non-redundant mediators of the neovascularization process elicited by the growth factor. Indeed, FGF2-triggered angiogenesis is significantly reduced in the CAM assay by mechanistically distinct steroidal (hydrocortisone) and non-steroidal (ketoprofen) anti-inflammatory drugs and by the pan-chemokine inhibitor M3. Also, FGF2 elicits a decreased angiogenic response in PI3K$\gamma^{-/-}$ mice exhibiting defective leucocyte migration and in clodronate-pre-treated, macrophage-depleted animals.

Monocytes/macrophages are active players in pathological angiogenesis [33–35]. They often precede, temporally and spatially, new vessel formation by altering the microenvironment, thus promoting vascular sprouting [36] and the recruitment of endothelial cell precursors [32]. Accordingly, we have observed that the early recruitment of mononuclear phagocytes (within 2–3 days after implantation) precedes blood vessel formation in FGF2-driven angiogenesis in the Matrigel plug assay. The depletion of monocytes/macrophages reduces also neovascularization driven by VEGF [37], placental growth factor (PlGF) [38] and IL-1β [39]. Thus, mononuclear phagocytes play a pivotal role in the angiogenesis process driven by various angiogenic growth factors, including FGF2.

Our observations indicate that FGF2-driven angiogenesis is, at least in part, chemokine-dependent. Chemotactic factors produced by FGF2-stimulated endothelium may recruit mononuclear phagocytes that, in turn, will amplify the angiogenic response by releasing

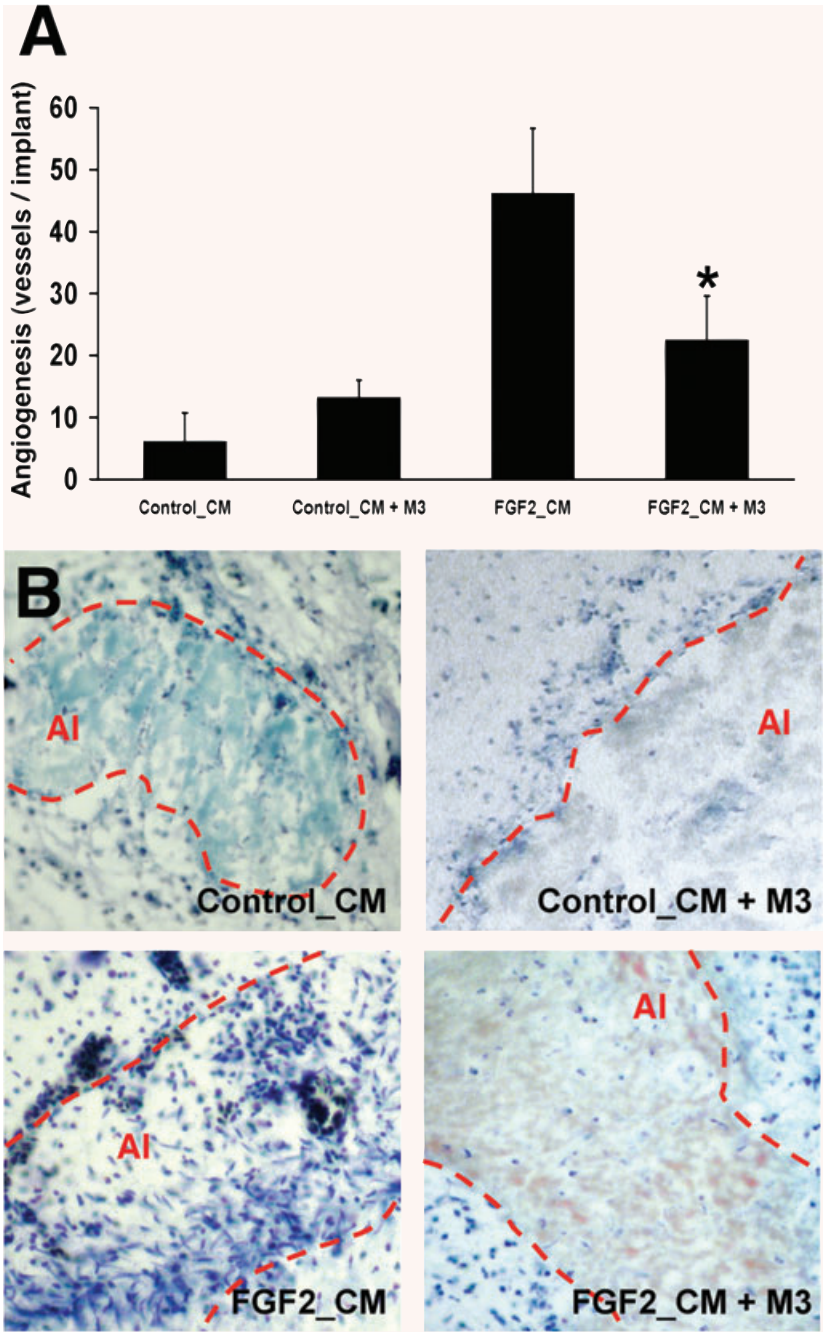

Fig. 7 The conditioned medium (CM) from FGF2-stimulated microvascular endothelial cells promotes chemokine-dependent angiogenesis *in vivo*. **(A)** Chick embryo CAM assay was performed with the CM from non-stimulated (Control_CM) and FGF2-stimulated (FGF2_CM) 1G11 endothelial cells in the absence or presence of 75 ng of the pan-chemokine inhibitor M3. Data are expressed as the mean ± SD of the number of vessels invading the alginate area (*, statistically different from the 'FGF2_CM' group, $P < 0.05$). (**B**) Representative histological sections of CAMs from the different experimental groups (May Grünwald-Giemsa staining). Note that FGF2_CM induces neovascularization and a strong inflammatory cell infiltrate within the alginate implant (AI, dotted line), both greatly reduced in the presence of M3.

monocyte-derived pro-angiogenic cytokines. Also, FGF2-induced chemoattractants may play a direct role in neovascularization by interacting with specific chemokine receptors expressed on endothelial cells [7]. Among them, the FGF2-induced chemokines Ccl2, Cxcl1, Cxcl16 and Cxc3l1 could act as enhancers of the neovascularization process elicited by the growth factor.

The capacity of the pan-chemokine inhibitor M3 [19] to inhibit angiogenesis triggered by FGF2 or by the CM from FGF2-stimulated endothelial cells is of interest. This gammaherpesvirus 68-derived protein prevents chemokine-mediated signal transduction and leucocyte recruitment induced by a number of chemokines and may have therapeutic potential in inflammatory conditions [40]. Our findings suggest that M3 protein may represent the basis for the design of novel angiogenesis inhibitors with therapeutic implications in angiogenesis-dependent pathological conditions, including tumour growth and metastasis.

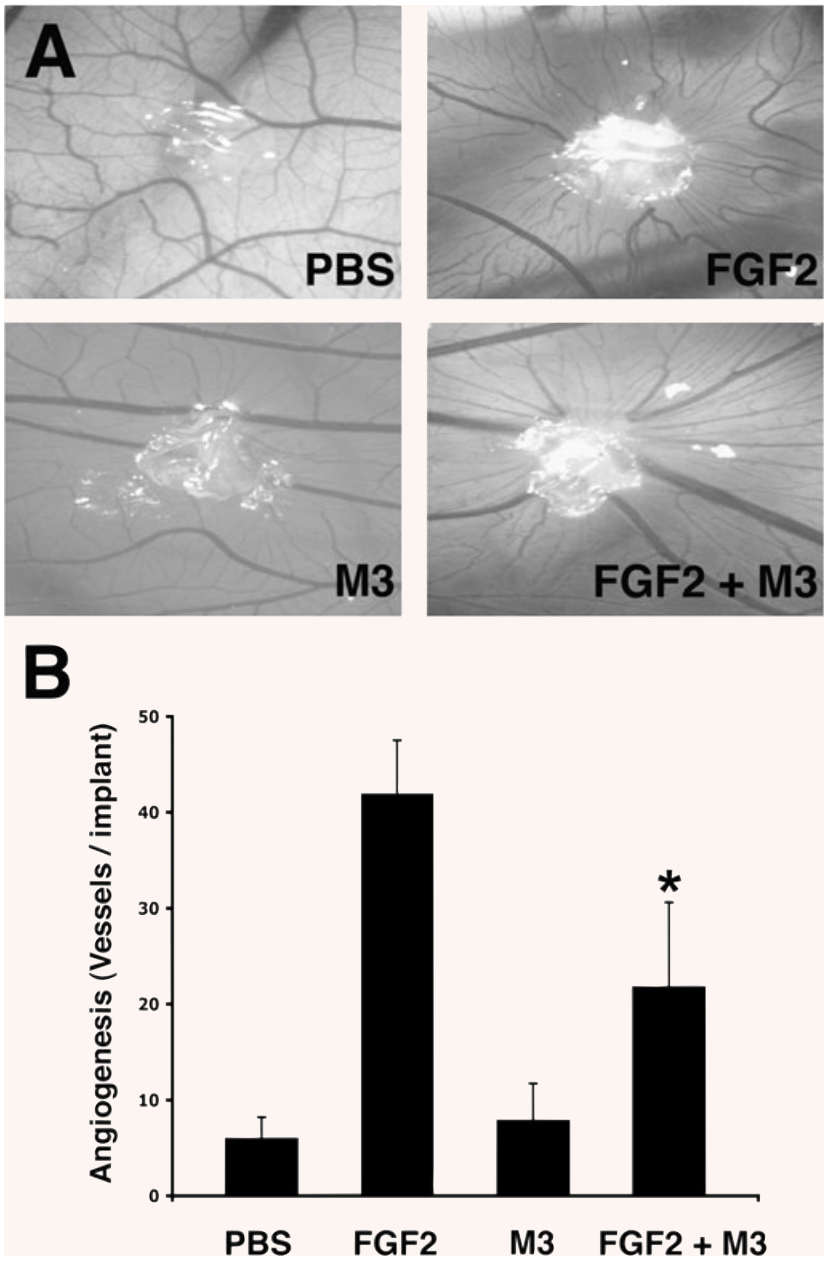

Fig. 8 Pan-chemokine inhibitor M3 impairs FGF2-induced angiogenesis. CAMs were implanted at day 11 of development with alginate beads containing vehicle (PBS), 150 ng of FGF2, 75 ng of M3 or 150 ng of FGF2 added with 75 ng of M3. After 3 days, CAMs were photographed (**A**, original magnification ×5) and angiogenesis was quantified by counting the number of microvessels (mean ± SD) invading the alginate area (**B**). Note the significant reduction (*, $P < 0.05$) in the number of newly-formed microvessels converging towards the FGF2 implant in the presence of the M3 inhibitor.

Taken together, our findings support the notion that monocytes/macrophages and inflammation-related gene products actively participate in the angiogenic process elicited by FGF2 as part of a complex cascade of cellular and molecular events triggered by the growth factor on microvascular endothelium. Indeed, FGF2 up-regulates also the expression of a variety of angiogenic growth factors in endothelial cells, including FGF2 itself (Table 4). This suggests that FGF2 is able to activate an autocrine loop of amplification of the angiogenic response that, together with the paracrine activity exerted by endothelium-derived cytokines/chemokines on inflammatory cells, will contribute to the modulation of the neovascularization process triggered by the growth factor.

Like FGF2, also VEGF is known to up-regulate the expression of pro-inflammatory mediators in endothelial cells [41–43]. In our experiments, the induction of inflammation-related genes by FGF2 represents an early event, most of these genes being up-regulated 1 hr after treatment (see Fig. 1). This precedes the limited increase of VEGF expression induced by FGF2 in 1G11 cells that reaches a maximal twofold up-regulation at 24 hrs after stimulation

(data not shown). This observation appears to rule out the possibility that the pro-inflammatory signature triggered by FGF2 in endothelial cells may represent an indirect, VEGF-mediated effect. On the other hand, in parallel with a significant monocyte/macrophage infiltrate, we have observed a sixfold increase of VEGF mRNA levels in FGF2-Matrigel plugs when compared to control implants (data not shown). Further experiments are required to fully dissect the complex cross-talk between FGF2 and VEGF during angiogenesis (reviewed in [13]).

FGF2 expression is augmented at sites of chronic inflammation, tissue injury and in human cancer [13]. Our observations suggest that FGF2 released after tissue damage may contribute to the host defence responses by activating pro-angiogenic and pro-inflammatory signatures in endothelium that, by acting in concert, will lead to neovessel formation and monocyte/macrophage engagement. Accordingly, *Fgf2*-null mice exhibit delayed wound repair [44] and neutralizing anti-FGF2 antibodies inhibit angiogenesis and formation of granulation tissue in a rat model of wound healing [45]. Conversely, local application of FGF2 effectively improves wound repair [46], the healing process being accompanied by mononuclear cell infiltrate recruitment [47]. On the other hand, long-term stimulation by FGF2 inhibits monocyte/macrophages adhesion to endothelium and the chemotactic response to various chemokines [48], suggesting that the pro- or anti-inflammatory activity of FGF2 may be contextual (discussed in [13]).

In conclusion, our findings point to inflammatory chemokines as important early mediators of FGF2-driven angiogenesis and indicate a relevant role for inflammatory cells in the neovascularization process elicited by the growth factor. Conversely, FGF2 may exert important functions at sites of inflammation and/or tissue injury not only by inducing neovascularization but also by contributing to the activation of innate immune responses.

Acknowledgements

This work was supported by grants from Istituto Superiore di Sanità (Oncotechnological Program), Ministero dell'Istruzione, Università e Ricerca (Centro di Eccellenza per l'Innovazione Diagnostica e Terapeutica, Cofin projects), Associazione Italiana Ricerca sul Cancro, Fondazione Berlucchi, NOBEL Project Cariplo, and Integrated European Commission Project STROMA to M.P. G.A. was supported by a Marie Curie Fellowship from the European Community Quality of Life Programme. A.A. was funded by the Wellcome Trust.

References

1. **Jackson JR, Seed MP, Kircher CH, *et al.*** The codependence of angiogenesis and chronic inflammation. *FASEB J.* 1997; 11: 457–65.
2. **Carmeliet P, Jain RK.** Angiogenesis in cancer and other diseases. *Nature.* 2000; 407: 249–57.
3. **Zijlstra A, Seandel M, Kupriyanova TA, *et al.*** Proangiogenic role of neutrophil-like inflammatory heterophils during neovascularization induced by growth factors and human tumor cells. *Blood.* 2006; 107: 317–27.
4. **Pober JS, Sessa WC.** Evolving functions of endothelial cells in inflammation. *Nat Rev Immunol.* 2007; 7: 803–15.
5. **Danese S, Dejana E, Fiocchi C.** Immune regulation by microvascular endothelial cells: directing innate and adaptive immunity, coagulation, and inflammation. *J Immunol.* 2007; 178: 6017–22.
6. **Williams CS, Mann M, DuBois RN.** The role of cyclooxygenases in inflammation, cancer, and development. *Oncogene.* 1999; 18: 7908–16.
7. **Romagnani P, Lasagni L, Annunziato F, *et al.*** CXC chemokines: the regulatory link between inflammation and angiogenesis. *Trends Immunol.* 2004; 25: 201–9.
8. **Voronov E, Shouval DS, Krelin Y, *et al.*** IL-1 is required for tumor invasiveness and angiogenesis. *Proc Natl Acad Sci USA.* 2003; 100: 2645–50.
9. **Naldini A, Leali D, Pucci A, *et al.*** Cutting edge: IL-1beta mediates the proangiogenic activity of osteopontin-activated human monocytes. *J Immunol.* 2006; 177: 4267–70.
10. **Leali D, Dell'Era P, Stabile H, *et al.*** Osteopontin (Eta-1) and fibroblast growth factor-2 cross-talk in angiogenesis. *J Immunol.* 2003; 171: 1085–93.
11. **Aplin AC, Gelati M, Fogel E, *et al.*** Angiopoietin-1 and vascular endothelial growth factor induce expression of inflammatory cytokines before angiogenesis. *Physiol Genomics.* 2006; 27: 20–8.
12. **Angelo LS, Kurzrock R.** Vascular endothelial growth factor and its relationship to inflammatory mediators. *Clin Cancer Res.* 2007; 13: 2825–30.
13. **Presta M, Dell'Era P, Mitola S, *et al.*** Fibroblast growth factor/fibroblast growth factor receptor system in angiogenesis. *Cytokine Growth Factor Rev.* 2005; 16: 159–78.
14. **Cross MJ, Claesson-Welsh L.** FGF and VEGF function in angiogenesis: signalling pathways, biological responses and therapeutic inhibition. *Trends Pharmacol Sci.* 2001; 22: 201–7.
15. **Zittermann SI, Issekutz AC.** Basic fibroblast growth factor (bFGF, FGF-2) potentiates leukocyte recruitment to inflammation by enhancing endothelial adhesion molecule expression. *Am J Pathol.* 2006; 168: 835–46.
16. **Wempe F, Lindner V, Augustin HG.** Basic fibroblast growth factor (bFGF) regulates the expression of the CC chemokine monocyte chemoattractant protein-1 (MCP-1) in autocrine-activated endothelial cells. *Arterioscler Thromb Vasc Biol.* 1997; 17: 2471–8.
17. **Kage K, Fujita N, Oh-hara T, *et al.*** Basic fibroblast growth factor induces cyclooxygenase-2 expression in endothelial cells derived from bone. *Biochem Biophys Res Commun.* 1999; 254: 259–63.
18. **Gualandris A, Urbinati C, Rusnati M, *et al.*** Interaction of high-molecular-weight basic fibroblast growth factor with endothelium: biological activity and intracellular fate of human recombinant M(r) 24,000 bFGF. *J Cell Physiol.* 1994; 161: 149–59.
19. **Parry CM, Simas JP, Smith VP, *et al.*** A broad spectrum secreted chemokine binding protein encoded by a herpesvirus. *J Exp Med.* 2000; 191: 573–8.
20. **Dong QG, Bernasconi S, Lostaglio S, *et al.*** A general strategy for isolation of endothelial cells from murine tissues. Characterization of two endothelial cell

lines from the murine lung and subcutaneous sponge implants. *Arterioscler Thromb Vasc Biol.* 1997; 17: 1599–604.
21. **Irizarry RA, Bolstad BM, Collin F, *et al.*** Summaries of Affymetrix GeneChip probe level data. *Nucleic Acids Res.* 2003; 31: e15.
22. **Dennis G Jr, Sherman BT, Hosack DA, *et al.*** DAVID: Database for Annotation, Visualization, and Integrated Discovery. *Genome Biol.* 2003; 4: P3.
23. **Rusnati M, Tanghetti E, Dell'Era P, *et al.*** alphavbeta3 integrin mediates the cell-adhesive capacity and biological activity of basic fibroblast growth factor (FGF-2) in cultured endothelial cells. *Mol Biol Cell.* 1997; 8: 2449–61.
24. **Hirsch E, Katanaev VL, Garlanda C, *et al.*** Central role for G protein-coupled phosphoinositide 3-kinase gamma in inflammation. *Science.* 2000; 287: 1049–53.
25. **Zeisberger SM, Odermatt B, Marty C, *et al.*** Clodronate-liposome-mediated depletion of tumour-associated macrophages: a new and highly effective antiangiogenic therapy approach. *Br J Cancer.* 2006; 95: 272–81.
26. **Knoll A, Schmidt S, Chapman M, *et al.*** A comparison of two controlled-release delivery systems for the delivery of amiloride to control angiogenesis. *Microvasc Res.* 1999; 58: 1–9.
27. **Montero A, Okada Y, Tomita M, *et al.*** Disruption of the fibroblast growth factor-2 gene results in decreased bone mass and bone formation. *J Clin Invest.* 2000; 105: 1085–93.
28. **Naganawa T, Xiao L, Abogunde E, *et al.*** *In vivo* and *in vitro* comparison of the effects of FGF-2 null and haplo-insufficiency on bone formation in mice. *Biochem Biophys Res Commun.* 2006; 339: 490–8.
29. **Bastaki M, Nelli EE, Dell'Era P, *et al.*** Basic fibroblast growth factor-induced angiogenic phenotype in mouse endothelium. A study of aortic and microvascular endothelial cell lines. *Arterioscler Thromb Vasc Biol.* 1997; 17: 454–64.
30. **Van Rooijen N, Sanders A.** Liposome mediated depletion of macrophages: mechanism of action, preparation of liposomes and applications. *J Immunol Methods.* 1994; 174: 83–93.
31. **Tanghetti E, Ria R, Dell'Era P, *et al.*** Biological activity of substrate-bound basic fibroblast growth factor (FGF2):s recruitment of FGF receptor-1 in endothelial cell adhesion contacts. *Oncogene.* 2002; 21: 3889–97.
32. **Anghelina M, Krishnan P, Moldovan L, *et al.*** Monocytes/macrophages cooperate with progenitor cells during neovascularization and tissue repair: conversion of cell columns into fibrovascular bundles. *Am J Pathol.* 2006; 168: 529–41.
33. **Dirkx AE, Oude Egbrink MG, Wagstaff J, *et al.*** Monocyte/macrophage infiltration in tumors: modulators of angiogenesis. *J Leukoc Biol.* 2006; 80: 1183–96.
34. **Sunderkotter C, Steinbrink K, Goebeler M, *et al.*** Macrophages and angiogenesis. *J Leukoc Biol.* 1994; 55: 410–22.
35. **Rehman J, Li J, Orschell CM, *et al.*** Peripheral blood "endothelial progenitor cells" are derived from monocyte/macrophages and secrete angiogenic growth factors. *Circulation.* 2003; 107: 1164–9.
36. **Moldovan NI, Goldschmidt-Clermont PJ, Parker-Thornburg J, *et al.*** Contribution of monocytes/macrophages to compensatory neovascularization: the drilling of metalloelastase-positive tunnels in ischemic myocardium. *Circ Res.* 2000; 87: 378–84.
37. **Cursiefen C, Chen L, Borges LP, *et al.*** VEGF-A stimulates lymphangiogenesis and hemangiogenesis in inflammatory neovascularization *via* macrophage recruitment. *J Clin Invest.* 2004; 113: 1040–50.
38. **Pipp F, Heil M, Issbrucker K, *et al.*** VEGFR-1-selective VEGF homologue PlGF is arteriogenic: evidence for a monocyte-mediated mechanism. *Circ Res.* 2003; 92: 378–85.
39. **Nakao S, Kuwano T, Tsutsumi-Miyahara C, *et al.*** Infiltration of COX-2-expressing macrophages is a prerequisite for IL-1 beta-induced neovascularization and tumor growth. *J Clin Invest.* 2005; 115: 2979–91.
40. **Fallon PG, Alcami A.** Pathogen-derived immunomodulatory molecules: future immunotherapeutics? *Trends Immunol.* 2006; 27: 470–6.
41. **Reinders ME, Sho M, Izawa A, *et al.*** Proinflammatory functions of vascular endothelial growth factor in alloimmunity. *J Clin Invest.* 2003; 112: 1655–65.
42. **Kim I, Moon SO, Kim SH, *et al.*** Vascular endothelial growth factor expression of intercellular adhesion molecule 1 (ICAM-1), vascular cell adhesion molecule 1 (VCAM-1), and E-selectin through nuclear factor-kappa B activation in endothelial cells. *J Biol Chem.* 2001; 276: 7614–20.
43. **Abe M, Sato Y.** cDNA microarray analysis of the gene expression profile of VEGF-activated human umbilical vein endothelial cells. *Angiogenesis.* 2001; 4: 289–98.
44. **Ortega S, Ittmann M, Tsang SH, *et al.*** Neuronal defects and delayed wound healing in mice lacking fibroblast growth factor 2. *Proc Natl Acad Sci USA.* 1998; 95: 5672–7.
45. **Broadley KN, Aquino AM, Woodward SC, *et al.*** Monospecific antibodies implicate basic fibroblast growth factor in normal wound repair. *Lab Invest.* 1989; 61: 571–5.
46. **Tsuboi R, Rifkin DB.** Recombinant basic fibroblast growth factor stimulates wound healing in healing-impaired db/db mice. *J Exp Med.* 1990; 172: 245–51.
47. **Ribatti D, Nico B, Vacca A, *et al.*** Endogenous and exogenous fibroblast growth factor-2 modulate wound healing in the chick embryo chorioallantoic membrane. *Angiogenesis.* 1999; 3: 89–95.
48. **Zhang H, Issekutz AC.** Down-modulation of monocyte transendothelial migration and endothelial adhesion molecule expression by fibroblast growth factor: reversal by the anti-angiogenic agent SU6668. *Am J Pathol.* 2002; 160: 2219–30.